A dopamine-gated learning circuit underpins reproductive state-dependent odor preference in *Drosophila* females

Ariane C. Boehm[a,b] , Anja B. Friedrich[a], Sydney Hunt[a], Paul Bandow[a,b,e], K.P. Siju[a], Jean-Francois De Backer[a], Julia Claussen[a] , Marie-Helen Link[a,f], Thomas F. Hofmann[c,d], Corinna Dawid[c,d] , Ilona C. Grunwald Kadow[a,b,c,e]

a Technical University Munich, School of Life Sciences, Neuronal Control of Metabolism, Freising, Germany
b Graduate School of Systemic Neurosciences, Ludwig Maximilian University, Martinsried, Germany
c ZIEL – Institute for Food and Health, Technical University Munich, School of Life Sciences, Freising, Germany
d Technical University Munich, School of Life Sciences, Chair of Food Chemistry and Molecular Sensory Science, Freising, Germany
e University of Bonn, Faculty of Medicine, Institute of Physiology II, Nussallee 11, 53115 Bonn, Germany
f Max Planck School of Cognition, Stephanstrasse 1a, Leipzig, Germany

Corresponding author: Ilona C. Grunwald Kadow, ilona.grunwald@uni-bonn.de

ABSTRACT

Motherhood induces a drastic, sometimes long-lasting, change in internal state and behavior in most female animals. How a change in reproductive state or the discrete event of mating modulates specific female behaviors is still incompletely understood. Using calcium imaging of the whole brain of *Drosophila* females, we find that mating does not induce a global change in brain activity. Instead, we find that mating modulates the pheromone response of β'1 dopaminergic neurons innervating the fly's learning and memory center, the mushroom body (MB). Using the mating-induced increased attraction to the odor of important nutrients, polyamines, we show that disruption of the female fly's ability to smell, for instance the pheromone cVA, during mating leads to a reduction in polyamine preference for days later indicating that the odor environment at mating lastingly influences female perception and choice behavior. Moreover, β'1 dopaminergic neurons are sufficient to replace mating experience in virgin females inducing the lasting behavioral increase in polyamine preference. We further show that MB output neurons (MBON) of the β'1 compartment are activated by pheromone odor and their activity during mating bidirectionally modulates preference behavior in mated and virgin females. Their activity is not required, however, for the expression of polyamine attraction. Instead, inhibition of another type of MBON innervating the β'2 compartment enables expression of high polyamine attraction. Taken together, our data in the fly suggests that mating-related sensory experience regulates female odor perception and expression of choice behavior through a dopamine-gated learning circuit.

Keywords:
Female behavior, reproductive state, mushroom body, lateral horn, modulation, polyamine, *Drosophila melanogaster*

INTRODUCTION

External stimuli and internal states guide decisions by influencing interpretation of the environment. These decisions not only impact on the individual itself but may have severe effects on its offspring. A female animal, therefore, adapts her choices to her reproductive state. This includes not only the decision to mate, but also a preference for certain, nutrient-rich food sources or, in case of egg-laying animals, oviposition sites (Chapman & Wolfner, 2017; Sayin, Boehm, Kobler, De Backer, & Grunwald Kadow, 2018). Choices pertaining to food, nutrients or egg-laying sites frequently depend on chemosensory cues such as odors or tastes. In line with this, changes in olfactory and gustatory perception have been reported for pregnant women (Ochsenbein-Kolble, von Mering, Zimmermann, & Hummel, 2007). The cellular and neural mechanisms responsible for such reproductive state-dependent preferences remain incompletely understood. A powerful mechanism for adapting preference for an odor or taste according to internal state acts within the very sensory neurons that detect the chemical (Leinwand & Chalasani, 2011). For instance, hunger increases the sensitivity of sweet taste and quenches that of bitter taste neurons in different animal species including humans (Carnell, Gibson, Benson, Ochner, & Geliebter, 2012; Chu, Chui, Mann, & Gordon, 2014; LeDue et al., 2016; Palouzier-Paulignan et al., 2012; Rolls, 2007). The estrous cycle influences how a female mouse perceives a putative mate (Dey et al., 2015). Outside of estrus, the hormone progesterone strongly inhibits the female's male pheromone-sensitive olfactory sensory neurons (OSNs), and thereby, completely blunts her interest in males. Moreover, previous results using volume measurements in human females before, during and after pregnancy suggested that pregnancy induces long-lasting, global changes in grey matter volume in several brain regions (Hoekzema et al., 2017), indicative of modulation in multiple higher brain regions. In the genetically tractable insect, *Drosophila melanogaster*, reproductive state also induces dramatic shifts in the female's chemosensory perception and choices (Gou, Liu, Guntur, Stern, & Yang, 2014; Hussain, Ucpunar, Zhang, Loschek, & Grunwald Kadow, 2016; Ribeiro & Dickson, 2010; Walker, Corrales-Carvajal, & Ribeiro, 2015). We have previously shown that a mating-induced transient neuropeptidergic modulation of OSNs strongly increases a female fly's preference for higher concentrations of polyamines, a nutrient that significantly increases female egg production (Hussain, Ucpunar, et al., 2016; Hussain, Zhang, et al., 2016). This rather short-lasting sensory modulation (~ 24 h) leads to a longer lasting change in the female's choice behavior, indicating that mating might modulate higher chemosensory processing in the female's central brain. Here, we aimed at investigating the nature and circuit mechanisms of these mating-induced longer lasting behavioral changes.

Reproductive state-dependent behavior of flies to polyamines is well suited to address this question. Polyamines, namely putrescine, spermine and spermidine, play essential and conserved roles in most eukaryotic cells and organisms, ranging from DNA replication, cell proliferation, embryonic development to healthy aging (Miller-Fleming, Olin-Sandoval, Campbell, & Ralser, 2015). High concentrations of putrescine in food increase egglaying in Drosophila females (Hussain, Zhang, et al., 2016). More importantly, olfactory detection of polyamines is relatively well characterized at the sensory neuron level and depends on two co-expressed ionotropic receptors (IR), IR76b and IR41a on the fly's antenna (Hussain, Zhang, et al., 2016; Silbering et al., 2011). Within the first several hours after mating, the expression of the neuropeptide receptor, sex peptide receptor (SPR) increases by tenfold in the OSNs leading, when bound to its ligand myoinhibitory peptide (MIP), to a depression of polyamine OSN presynaptic output to the second order neurons of the olfactory system (Hussain, Ucpunar, et al., 2016). While virgin flies show a high attraction toward low concentration of polyamines, mated flies are attracted to higher concentrations (Hussain, Ucpunar, et al., 2016).

Attraction to nutrients, egg-laying or nest building sites are considered innate behaviors in most female animals (Cury, Prud'homme, & Gompel, 2019). Innate olfactory behavior is thought to rely on stereotyped circuits connecting specific glomeruli in the antennal lobe (AL) to specific neurons in the lateral horn (LH) (Chin, Maguire, Huoviala, Jefferis, & Potter, 2018; Ebrahim et al., 2015; Min, Ai, Shin, & Suh, 2013). In line with this, previous work in the fly has implicated the LH in the control of reproductive behaviors, such as responses to sex pheromones (Jefferis et al., 2007; Ruta et al., 2010). Neurons innervating or providing output of the LH show largely stereotypic responses to odors (Frechter et al., 2019; Jeanne, Fisek, & Wilson, 2018). Moreover, recent studies implicated neurons in the LH in innate valence decisions and odor classification (Dolan et al., 2019; Jeanne et al., 2018; Strutz et al., 2014). Interestingly, modulation of innate behavior, for instance in the context of hunger, also involves the second higher olfactory brain center, the mushroom body (MB), a well-characterized brain region known for its role in associative memory formation (Bracker et al., 2013; Cohn, Morantte, & Ruta, 2015; Grunwald Kadow, 2018; Heisenberg, 2003; Krashes et al., 2009; Lewis et al., 2015; Sayin et al., 2018; Tsao, Chen, Lin, Yang, & Lin, 2018). In reproductive behavior, dopaminergic neurons (DANs) innervating the MB regulate the mated female's decision of where to lay her eggs (Azanchi, Kaun, & Heberlein, 2013). DAN odor responses are modulated by the mating state of the female (Siju et al., 2020). In addition, it is worth noting that a crucial role for dopamine and the MB have been shown in the mating induced changes in male courtship learning (Keleman et al., 2012; Siegel & Hall, 1979).

Here, we have investigated the neural circuits underpinning reproductive state-dependent female attraction to polyamines using brain-wide imaging, connectomics and behavioral analysis. Our combined data suggest that specific dopaminergic neurons relay the experience of mating to the female's MB, thereby inducing a long-lasting change in female olfactory preference.

RESULTS

Mating related signals induce a lasting increase in female polyamine attraction

Mated female flies show an increased attraction to polyamine odors, such as putrescine, as compared to virgin females due to SPR-mediated neuromodulation of polyamine sensitive OSNs (Hussain, Ucpunar, et al., 2016). The increased attraction, interestingly, lasts for at least 9 days after mating (Fig. 1A,B), while the neuromodulation of the OSNs appears to decline already several hours after mating (Hussain, Ucpunar, et al., 2016). We wondered how mating induces such a long-lasting change in olfactory preference in female flies.

It is possible that the same type of neuromodulation and lasting change also affects other olfactory behavior and odors. However, the attraction to the odor of ammonia, another odor released during decomposition of organic matter, did not increase significantly after mating (Fig. S1A).

During copulation the male fly transfers sperm and seminal fluid into the female reproductive tract. Among the factors transferred with the sperm is one of the ligands of SPR, sex peptide (SP). SP binds to neurons expressing SPR in the female's reproductive tract and induces the so-called canonical post-mating switch, a suite of behaviors associated with reproduction such as increase in egglaying and rejection of males attempting to mate (Kubli, 2003; Yapici, Kim, Ribeiro, & Dickson, 2008). Although SPR is required for the change in the mated female's polyamine preference behavior, this appears to rely mainly on the other ligands, myoinhibitory peptides (MIPs) (Hussain, Ucpunar, et al., 2016; Kim et al., 2010) as females mated to SP mutant males still undergo the change in polyamine preference behavior (Hussain, Ucpunar, et al.,

2016). Therefore, we next tested females mated to sterile males. There are two previously used experimental methods to achieve such an effect: males that do not produce either seminal fluid protein or sperm (Boswell & Mahowald, 1985; Chow, Avila, Clark, & Wolfner, 2015). To generate males incapable of producing seminal fluid protein, accessory glands were disrupted through induction of ER stress (see methods; *prd-GAL4;UAS-BiP-RNAi*). After copulation with a seminal fluid protein deficient male, females showed a normal increase in preference for polyamine odor as compared to controls (Fig. S1B). Similarly, copulation with sperm-deficient males, which were generated by using the male progeny of female mutants of *tudor* (Chapman et al., 2003), also led to mated females that behaved indistinguishable from females that mated with wildtype males (Fig. S1C). This result was in line with our previous finding (Hussain, Ucpunar, et al., 2016), and suggested that not only was SP not essential, but also that other sperm- and seminal fluid-associated factors were dispensable. To further support the conclusion that fertilization was not essential for the change in odor preference, we tested females that, similarly to females mated to sterile males, were unable to produce eggs by generating *ovoD* mutant females. *OvoD* females mated with wildtype males underwent the switch in behavior and were attracted to polyamines to the same extent as controls (Fig. S1D).

We continued to look for additional triggers that could work in synergy with courtship such as signals transferred or present during mating. Male flies perform a complex courtship before attempting to mount the female in order to mate. During this time, females will, among other signals, also smell male-emitted pheromones such as 11-cis-Vaccenyl acetate (cVA). We hypothesized that mating, or more specifically pheromone, could act as a contextual sensory signal able to lastingly modulate higher olfactory processing, perhaps analogous to other sensory contextual experiences such as sweet taste or pain. Thus, we imaged responses to cVA in dopaminergic neurons (DANs) innervating the MB, as DANs are instrumental in many behavioral adaptations including state-dependent changes and learning. *In vivo* 2-photon imaging revealed that some subsets of DANs responded strongly to cVA in a mating state-dependent manner suggesting (a) that cVA could act as a contextual signal and (b) that mating induces a lasting change cVA-induced DAN activity. Primarily, DANs innervating a specific compartment of the MB, β'1, responded significantly stronger to cVA in females days after mating as compared to virgins (Fig. 1C,D).

Interestingly, cVA and other pheromones (e.g. 7-tricosene) are transferred onto the female during courtship and mating, and remain on her body for an extended period of time (~24 h) (Ejima et al., 2007). To test the role of courtship and its signals *vs.* actual mating, we allowed fly couples to go through the courtship ritual but separated them just as the male attempted to mount the female. We then analyzed the odor preference behavior of these females that were technically still virgins. The behavior of these females lay between virgins and mated females and was neither significantly different from virgins nor from mated females consistent with the hypothesis that courtship related signals might contribute as behavioral change triggers (Fig. S1E). Based on this observation and our data above, we next tested one specific aspect of the courtship ritual, odor detection. Pheromone detection relies on the general OR co-receptor, ORCO, and different specific ORs. We thus analyzed mated females mutant for *ORCO*, and hence unable to smell pheromones among other odors. Importantly, ORCO is not required for the detection of polyamine odor, which is mediated by IR76b and IR41a (Hussain, Zhang, et al., 2016; Silbering et al., 2011). Mated *ORCO* mutant females displayed a significantly lower polyamine preference compared to controls (Fig. 1E).

Previous work showed that food odors also enhance courtship and mating (Grosjean et al., 2011), and that cVA promotes aggregation behavior of flies on food patches (Das et al., 2017; Lebreton et al., 2015).

Interestingly, polyamines are present in high concentrations in standard fly food: histamine (5.49), ethanolamine (676.65), phenylethylamine (5.16), putrescine (172.50), β-alanine (930.84), tyramine (166.64), spermidine (18120.77) and spermine (492.81) (Fig. S1F). Thus, the total amount of polyamines in standard fly food is ~20 mg in 100 g food, which is comparable to levels in very polyamine-rich foods such as oranges (Kalac, 2014). To test whether the presence of odors such as pheromones or polyamines was important during mating to induce a higher polyamine odor preference upon mating, we blocked the synaptic output of ORCO and IR76b/IR41a-expressing OSNs exclusively during the 24 h at and around mating (Fig. 1F). While synaptic inhibition of IR41a- and IR76b-expressing OSNs during mating had no effect on the mated female's odor preference, blocking the synaptic output of ORCO-OSNs during mating but not at test significantly reduced those females' attraction to the putrescine odor (Fig. 1F). Similarly, inhibition of synaptic output of cVA-responsive OR67d OSNs during mating but not during test reduced the mated female's attraction to putrescine (Fig. 1G). Thus, we analyzed whether the smell of cVA was sufficient to induce mated-like female polyamine preference by exposing virgin females in food vials for 24 h to cVA (50 µl pure solution) or just water on a filter paper. We detected no significant difference between the groups indicating that cVA alone is insufficient to induce mated female odor preference (Fig. S1G).

Next, to test whether the context of food was necessary for females to change their preference upon mating, we removed virgin females for 24 h from fly food and transferred them to a pure agarose substrate. We mated 50% of these females to males on agarose, while the other 50% remained alone – hence, they remained virgin – for the same amount of time. After these 24 h, flies were transferred again onto regular fly food. Virgins behaved as expected and showed no polyamine preference (Fig. S1H). Females mated on agarose showed no significant decrease in polyamine preference compared to females mated on regular fly food (Fig. S1H). We next raised and mated females on a holidic diet containing precise amounts of nutrients such as amino acids but no added polyamines (Piper et al., 2014). We again found no difference in the preference for polyamine odor between the two groups of mated females (Fig. S1I).
These results provide evidence that courtship promoting signals such as the pheromone cVA contribute to a switch in preference behavior, but that the presence of food odor, including polyamines, during mating is not required.

Mushroom body Kenyon cells mediate state-dependent polyamine attraction

Given the role of the MB in behavioral adaptations and our data above indicating a role of olfaction at the time of mating (see Fig. 1F), we wondered whether the MB was involved in the mating-induced increase in polyamine preference. We started with the principal cells of the MB, the Kenyon cells (KCs), which long axons form the MB lobes that are innervated by DANs and provide output to MB output neurons (MBONs). Given the role of olfaction in courtship and mating, we switched to single fly assays to ensure that mated females were indeed mated; all females were analyzed for successful fertilization upon mating and females that did not produce offspring were discarded from the analysis. We used a set of split-Gal4 lines, generated to target individual cell types of the MB network (Aso, Hattori, et al., 2014). We expressed the temperature-sensitive mutant of dynamin, Shibire^{ts1} (Kitamoto, 2001), in all KCs (*MB10B-Gal4;UAS-shits1*), inhibited synaptic transmission by shifting the females to 30℃, and tested their individual polyamine odor preference in the T-maze assay (Fig. 2A). KC output could be required for the expression of polyamine odor attraction but also for the increase from virgin to mated female behavior. To test this hypothesis, we shifted the females (*MB10B-Gal4;UAS-shi^{ts1}*) from 25 to 30℃ for 24 h at three different time points: (1) 24 h before mating, (2) 24 h during mating, (3) 24 h after mating, and (4) at test (Fig. 2A). Blocking synaptic output during 24 h before or between mating and test had no significant effect on the mated female's preference for

polyamines (Fig. 2B, 50% represents chance). However, blocking KC output exclusively during the 24 h during and around mating, completely prevented the change from virgin to mated female putrescine attraction (Fig. 2B). Inhibition of KC output during the choice test also reduced the percentage of single females choosing putrescine over water (Fig. 2A,B), suggesting an involvement of KC output for the expression of polyamine preference. By contrast, KC output did not affect the choice of virgins (Fig. 2B). Thus, KC synaptic output appears to be required at two timepoints: First, it is necessary to induce the change in behavior upon mating, and second, it influences the expression of the actual behavioral choice.

Together, these data suggest that MB KCs are required for the mating-induced change in female choice behavior and for decision-making.

Specific dopaminergic neurons can replace mating experience

Our data suggested that mating-related olfactory signals such as cVA are required to induce increased polyamine attraction after mating. Moreover, MB β'1-innervating DANs respond to cVA in a mating state-dependent manner. We next asked whether these state-dependent changes where specific to some neurons or whether mating would induce a more wide-spread or even global change in brain activity. For instance, recent evidence suggests that changes in hormone levels trigger circuit maturation in *Drosophila* flies during the first week of life (Leinwand & Scott, 2021). We used whole brain lightfield imaging to record the activity of all neurons in the brain in living female flies (*nsyb-Gal4;UAS-CaMP*) (Aimon, Cheng, Gjorgjieva, & Grunwald Kadow, 2022; Aimon et al., 2019; Woller, Bandow, Aimon & Grunwald Kadow, 2021) (Fig. S2A). Mating did not appear to change brain activity globally in 1-week old mated and virgin females stimulated with putrescine, and we did not find any significant brain-wide mating state-dependent changes (Fig. S2B,C). Similarly, we did not detect any significant differences between mated and virgin flies by analyzing individual brain regions (Fig. S2D,E). These data suggested that mating does not induce a significant global change in brain state (e.g. general arousal state), but rather relies on modulation of specific neurons and neural circuit elements relevant to a specific task.

Therefore, we sought to test experimentally whether DANs, in particular the DANs responsive to cVA, are involved in the mating-induced change in female polyamine preference. We started with line MB188B, because it labeled several PAM DANs with axons in the β'1 lobe, namely PAM-β'1ap and PAM-β'1m, as well as PAM-γ3, and PAM-γ4 (Aso, Hattori, et al., 2014). We manipulated the activity of these PAMs in virgin and mated females as a replacement for actual mating or during mating (Fig. 3). Given that β'1 DANs responded to cVA, we again used a single fly T-maze to be able to check every single female fly after an experiment for its mating state (i.e. eggs laid or not). Remarkably, neuronal activation of these DANs with TrpA1 was highly efficient in switching virgin female preference to mated female preference levels for polyamine (Fig. 3A) indicating that β'1 DANs can replace mating experience possibly due to their response to mating-related signals (see Fig. 1C,D). By contrast, inhibition of synaptic output of the same DANs had not effect (Fig. 3B) indicating that these DANs are sufficient but not strictly necessary for the preference increase. Surprisingly, activation of PAM-β'1 DANs during mating significantly reduced the mated female's attraction to polyamine (Fig. 3A). Therefore, it appears that β'1 DANs can bidirectionally modulate female choice behavior. This bidirectionality could possibly be achieved through alternative signaling pathways downstream of dopamine receptors as shown for associative learning (Handler et al., 2019).

In contrast to the bidirectional change in preference induced by activation of DANs innervating the β'1 lobe, the same paradigm with another line, MB109B that expresses in a set of β'2 DANs, did not induce changes

in mated or virgin fly behavior (Fig. S3E). Similarly, activation of most of the second cluster of DANs innervating the MB, the PPL1-DANs (MB60B) instead of mating, only induced a mild reduction in mated female preference, but had no effect on virgin female behavior (Fig. 3C), suggesting that the effect observed for β'1 DANs is specific to the context.

We next tested the involvement of these DANs in the expression of polyamine preference at the time of T-maze test. Thus, we expressed Shi^{ts1} in larger and smaller subsets of PAM- or PPL1-DANs using lines such as MB42B and MB60B, respectively. Inhibition of PAM-DAN synaptic output at the time of test had no effect on virgin behavior, but significantly reduced mated female attraction to putrescine (Fig. 3D, S3A-D). By contrast, inhibition of PPL1-DAN output resulted in an opposite phenotype; mated females were still highly attracted to the odor, but now also virgins showed a higher attraction to putrescine as compared to controls (Fig. S3F-I). These results are consistent with the interpretation that DANs regulate the expression of female putrescine attraction in a state-dependent manner; while PAM-DANs appear to be necessary for the expression of attraction of mated females, the activity of PPL1-DANs in virgins seems to suppress the expression of polyamine attraction.

The present data, therefore, provide support for an important role of DANs at two timepoints. First, DANs innervating the β'1 region of the MB bidirectionally modulate polyamine odor attraction at the time of mating. Second, other DANs including β'2 and γ4 (see Fig. 3D) promote the expression of mated female putrescine attraction, while PPL1-DANs repress this expression in virgins.

Specific MB output neurons are involved at different time points during reproductive state-dependent female decision-making

MBONs, as major output of MB KCs and targets of DANs, are involved in guiding valence-based action selection. Exogenous activation through optogenetics of selected MBONs elicits attraction or aversion, respectively, to light (Aso, Sitaraman, et al., 2014). In classical associative learning paradigms, DANs are thought to modulate the synapse between KC and MBON during learning and thereby change the weight between different MBONs such that the animal is more likely to express attraction vs. aversion (Owald & Waddell, 2015).

Given our imaging data and the effect of β'1-DAN activation instead of mating, we analyzed the role of MBON-β'1 (aka MBON10) (Li et al., 2020). Blocking of synaptic output of MBON-β'1 during the 24 h period around mating resulted in a strong and significant reduction of polyamine odor preference in mated females at the time of odor test (Fig. 4A). suggesting that this MBON's synaptic output critically contributes to the induction of mating-related behavioral changes. In line with this interpretation, dTrpA1-mediated activation of MBON-β'1 in virgins in place of mating significantly increased these females' polyamine preference at the time of choice (Fig. 4B). Interestingly, activation of MBON-β'1 in virgin females only at the time of choice also led to a significant increase in polyamine attraction compared to controls (Fig. S4A). This activation also reduced mated female attraction (Fig. S4A), which suggests a bidirectional role for this MBON at expression of choice, similar to the bidirectionality of the DANs innervating the same compartment during mating. In contrast to the PAM- β'1, however, output of the MBON-β'1 was required during mating (compare Fig. 3B and 4A) to induce an increased attraction to putrescine at the time of test in mated females. Inactivation of MBON-β'1 (*MB57B-Gal4;UAS-shi^{ts1}*) output at the time of olfactory test, by contrast, did not significantly reduce the mated female's preference for polyamine and also had no effect on virgin female behavior (Fig. 4C, S4B). Together, these results argue that MBON-β'1 and PAM- β'1 synaptic output modulate the degree of polyamine attraction at the time of mating.

In contrast to other MBONs, relatively little is known regarding the function of MBON-β'1 that would explain the observed behavioral phenotypes. MBON-β'1 releases GABA as neurotransmitter and might, therefore, inhibit downstream neuronal activity (Aso, Hattori, et al., 2014). We used the trans-TANGO system and EM connectomics to identify the putatively inhibited downstream neuron (Fig. S4D-F). Expression of trans-TANGO under the control of *MB057B-Gal4* primarily and repeatedly labeled a neuron with neurites in the β'2 region of the MB (Fig. S4E,E'). We identified a candidate neuron for our TANGO result using the EM connectome (Fig. S4D,F) (Li et al., 2020). PAM-β'2m (aka PAM06) receives direct input from MBON-β'1. PAM-β'2m in turn synapses onto MBONs providing output from the β'2 MB compartment (i.e. β′2mp, β′2mp_bilateral; Fig. S4F). Interestingly, β'2 MBONs (i.e. MBON- γ5β′2a) form direct input synapses on MBON-β'1 (Fig. S4F) suggesting a recurrent loop between the β'1, β'2 MBONs and DANs (Li et al., 2020). Such a recurrent loop could drive persistent behavioral changes as previously shown for male courtship memory (X. Zhao, Lenek, Dag, Dickson, & Keleman, 2018).

MBONs providing output from β'2 were shown to be required for hunger state-dependent odor aversion (Lewis et al., 2015; Owald et al., 2015). Moreover, activation of these MBONs using optogenetics is sufficient to elicit strong avoidance (Aso, Sitaraman, et al., 2014; Lewis et al., 2015). Based on these prior data, we postulated that MBON-β'1 and MBON-β'2 could modulate each other's activity through PAMs. To probe the involvement of β'2 MBONs in polyamine attraction, we chose line MB11B-Gal4, which drives Gal4 expression in three different MBON-types, namely MBON-β'2mp, MBON-β'2mp_bilateral and MBONγ5β'2a. Indeed, temporary thermogenetic activation of these MBONs (*MB11B-Gal4;UAS-dTrpA1*) at the time of olfactory choice, significantly reduced the mated female's attraction to polyamine (Fig. 4D). Temporary synaptic output inhibition at the time of choice in virgins increased their attraction to polyamine odor but did not affect the high attraction of mated females (Fig. 4F). By contrast, neither activation nor synaptic output inhibition at the time or in place of mating had an effect on the female's preference behavior (Fig. 4E, S4E). These data suggest that β'2 output is important for the expression of the choice, but in contrast to β'1 output, it is insufficient to induce the mating-induced change in choice behavior.

We thus propose a similar scenario as observed for associative learning with the experience of mating providing a contextual signal conveyed to the MB through the β'1 compartment. The β'2 compartment, like in expression of learned behavior, is only necessary to express attraction at the time the mating-induced preference is needed.

Calcium imaging of MBON activity before and after mating

We have shown that β'1 DANs are modulated mating. Moreover, our behavioral data suggested that β'1 MBONs play an important role in inducing mating state-dependent polyamine attraction. We used *in vivo* 2-photon calcium imaging to ask whether MBONs, like DANs, are modulated by the mating experience. Importantly, given a previous report that β'1 MBONs, in contrast to β'2 and other MBONs, respond only to selected odors, we tested their response to cVA and putrescine (Hige, Aso, Rubin, & Turner, 2015). To this end, we recorded GCaMP-reported calcium changes in response to odor stimulation (*MB57B-Gal4;UAS-GCaMP6f*) and found that this MBON indeed responded to the odor of cVA, but not to the odor of putrescine, in line with a more specific or selective role of this MBON (Fig. 5A-E). We next compared the response in virgins to the response in mated females 3-5 days after mating as done for the behavior. We did not find a significant difference between the response to cVA in virgins as compared to mated females (Fig. 5E). In addition, neither MBON of virgins nor of mated females responded significantly higher to putrescine

than to water (Fig. 5E). These data indicated that β'1 MBONs are responsive to cVA and that mating does not lead to a modulation of this response that lasts for several days after mating.

Associative learning, i.e., association of a shock with an odor, modulates the response of β'2 MBONs (Owald et al., 2015). We used the same setup as above to investigate the response of the β'2 MBONs before and after mating. In contrast to β'1 MBONs, these MBONs responded equally strong to putrescine and cVA (Fig. 5F-H). Different from our predictions, we again found no evidence for a long-lasting mating-induced modulation of these odor responses (Fig. 5H).

Given that β'1 MBON output is necessary during mating and not during test it is possible that any short-term modulation has disappeared at the time of our imaging. We therefore tested the effect of exogenous activation of PAM β'1 DANs, which is sufficient to induce a high polyamine attraction in virgins, on β'1 and β'2 MBONs (Fig. S5). We optogenetically activated β'1 DANs with pulsing light for 24 h using CsChrimson and recorded calcium responses in the β'1 and β'2 MBONs to putrescine odor thereafter (*MB188B-Gal4;UAS-CsChrimson; VT1211-lexA;lexAop-GCaMP7f*). Imaging following this exogenous activation again did not reveal a difference in polyamine responses between the test group and the controls (Fig. S5).

Based on the behavioral data, we predicted and found that MBON β'1 would respond to cVA. We also predicted that mating or the exogenous activation of β'1-PAMs would lead to a lasting response of the β'2-MBONs, similar to what was shown upon learning. However, we did not observe a change in the response of β'1 or β'2 MBONs to putrescine upon mating or β'1-PAM activation. At this point, we can only speculate that the paradigm, in particular the temporal aspect and the fact that β'1-PAMs bidirectionally modulate the behavior of virgin and mated females, respectively, is complex and that changes might be found downstream of the MB or are more subtle and thus difficult to detect with calcium indicators.

Specific lateral horn output neurons mediate attraction to polyamines

Given the previously reported role of the LH in the expression of learned behavior (Dolan et al., 2018), we also analyzed candidate neurons in this brain structure for their role in the expression of polyamine attraction in mated females. Projection neurons (PNs) project from the antennal lobe (AL) glomerulus (VC5), where they receive input by the OSNs detecting polyamine odors (i.e. IR41a/IR76b OSNs) to the LH and the MB calyx (Fig. S6A-B'). As the number of LH output neurons (LHONs) is large, we used the lightfield imaging data (see Fig. S2) to narrow down the putative anatomy of candidate neurons (Fig. 6A, *nsyb-Gal4;UAS-GCaMP6m*). Stimulation of mated females with putrescine elicited a clear increase in GCaMP fluorescence mainly in the ventral, but also in a smaller area in the dorsal, region of the LH (Fig. 1A). By contrast, stimulation with 1% vinegar activated primarily neurons in the dorsal part of the LH (Fig. 1A) as previously observed (Strutz et al., 2014). This suggested that putative polyamine-responding LHONs strongly innervate the ventral portion of the LH. We again used EM connectomics to search for LHNs receiving input from VC5 PNs in the electron microscope connectome of a female hemibrain (Fig. 1B-D, S6C) (Li et al., 2020; Scheffer et al., 2020). According to neuPrint, three different types of PNs receive direct input from the VC5 glomerulus, adPN, lvPN, and l2PN. Only one of these types, adPN, innervates both the LH and the MB calyx. The primary LHON type receiving adPN input is AD1b2 (Fig. S6C). Most AD1b2 dendrites are indeed located in the ventral part of the LH (Fig. 6C,D). To test the function of putative LHNs more directly in polyamine attraction of mated females, we selected several LHN split-Gal4 lines that labeled AD1b2, but also LHNs that were not directly connected to VC5 PNs (Dolan et al., 2019).

Using these LHN split-Gal4 lines, we temporally blocked synaptic output with Shi^{ts1} during test (Fig. 6F). Only two lines showed a significant reduction (Fig. 6E). One of these lines, L1779, strongly labeled several neurons of the AD1b2 type suggesting that the observed synaptic connections are indeed relevant for the attraction of putrescine. Two additional lines that also expressed in AD1b2 neurons, by contrast, did not reduce putrescine attraction significantly (Fig. 6E). These lines, however, labeled fewer neurons than L1779 suggesting a certain redundancy between the AD1b2 type neurons (Fig. S6E-G; L1538/1539: 9.8±1.5 *vs.* L1779: 19.3±2.6, $p<0.001$). Of note, AD1b2 neurons provide direct and indirect synaptic input to the β'1 compartment of the MB (Fig. 6F).

Interestingly, expression of Shi^{ts1} under the control of line L1614, which labels the aSP-g neuron, also significantly reduced the attraction to putrescine (Fig. 6E). The aSP-g neuron receives input from the DA1 glomerulus (Fig. S6D), which in turn receives input by the male pheromone cVA-detecting OSNs. This result is in line with the reduction in polyamine attraction observed by inactivation of ORCO- and OR67d-expressing OSNs (see Fig. 1). Moreover, similar to AD1b2, aSP-g neurons provide indirect input to DANs innervating the β'1 MB-compartment (Fig. S1H,I), which play a critical role in modulating female attraction to polyamines (see Fig. 3A).

Altogether, these data indicate that multiple LHONs are involved in the mated female's attraction to polyamines, including AD1b2, which receives strong synaptic input by one type of VC5 PN, and aSP-g neurons, which are activated by cVA as well as some other odors (Kohl, Ostrovsky, Frechter, & Jefferis, 2013).

DISCUSSION

The transition from a sexually immature to a mature, reproducing parent is a major step in the life of most animals. With this step come new needs and demands, reflected in a significant change in an animal's behavior and preferences. While many aspects of reproductive behavior are innate, sexual and parental behavior is highly flexible and changes through physiology and with experience (Griffith & Ejima, 2009; Koch & Ehret, 1989; Marlin, Mitre, D'Amour J, Chao, & Froemke, 2015). In addition, sexually mature animals spend a major proportion of their lives with generating or caring for their offspring. In line with this, some of the behavioral and neuronal changes persist for a significant fraction of an animal's lifespan (Hoekzema et al., 2017; Insel, Preston, & Winslow, 1995; Reisenman, Riffell, & Hildebrand, 2009; M. Zhao, Garland, Chappell, Andrew, & Saltzman, 2017).

Here, we have identified a mechanism how a change in reproductive state translates into behavioral output. We propose a model wherein mating experience, through the sensation of mating-related odors such as cVA, is relayed to the MB via specific DANs innervating the β'1 compartment. Activation of β'1-DANs in turn modulates the output of β'1 MBONs inducing a higher polyamine preference upon mating (Fig. 7). The expression of this higher preference relies on β'2 MBONs and LHONs, analogous to the situation found upon associative learning (Dolan et al., 2018). Thus, changes induced by the experience of mating are induced and expressed through a dopamine-gated learning circuit.

Triggers for reproductive state-dependent changes in the female brain

We have previously shown that SP appears to play a rather redundant role in the increase in polyamine attraction (Hussain, Ucpunar, et al., 2016). Instead, SPR in OSNs together with its conserved ligand MIP depress OSN synaptic output upon mating and thereby reduce OSN sensitivity to polyamines. Similarly, mating also reduces the response of the DA1 glomerulus to cVA (Lebreton et al., 2014). How this translates into a higher response of β'1 DANs to cVA is unclear and probably lies within the complex circuit structure

of the MB. Nevertheless, the combined evidence indicates a mating-induced modulation of early as well as higher olfactory processing.

Our data reported here is consistent with the interpretation that olfactory signals related to mating are involved in conveying mating experience to the MB as transient blocking of synaptic output of ORCO-dependent OSNs during mating reduced the mated females' attraction at the time of test, suggesting that OR-dependent odor detection during mating, for instance male pheromone, contributes to the change in behavior from virgin to mated female. Of note, males transfer some of their pheromone onto the female during copulation (Keleman et al., 2012), and they also mark feeding and oviposition sites for females by depositing pheromone (Lin, Prokop-Prigge, Preti, & Potter, 2015), suggesting that pheromones are present in the female's environment just before, during and sometime after mating (Ejima et al., 2007). By contrast, the presence of polyamines during mating was not required as temporal inhibition of polyamine OSN synaptic output during mating did not affect the mated female's high putrescine attraction during test. In line with a putative role of odors such as pheromones, *in vivo* calcium imaging data shows that the pheromone cVA activates DANs and MBONs of the β'1 compartment; this activation is modulated by state (Siju et al., 2020). We speculate, that the mechanisms we describe here might represent a female version of male courtship learning (Ejima et al., 2007; Keleman et al., 2012). Consistent with our observations, specific DANs can mimic courtship experience in naive males in the absence of an actual rejection by an already mated female (Keleman et al., 2012). Males likely associate cVA, which was transferred during previous copulation by another male onto the female, with the experience of rejection by an already mated female (Ejima et al., 2007). In our scenario, the pheromones transferred to the female during copulation would be 'sensed' by the β'1 DANs which in turn induce a shift in how the MB regulates the expression of polyamine odor preference (Fig. 7).

Naturally, mating itself stimulates also mechanosensory neurons in the female's reproductive tract and thereby appears to contribute to a switch in her behavior (Gou et al., 2014; Shao et al., 2019). Other hormonal or peptidergic signals, such as steroids or juvenile hormone (JH) could play a role (Moshitzky et al., 1996). For instance, JH drives network maturation of the MB in young flies and thereby promotes their ability to form memories (Leinwand & Scott, 2021). Recent elegant work showed that mating triggers neuropeptide (i.e. Bursicon) release from enteroendocrine cells, which in turn modulate female appetite (Hadjieconomou et al., 2020). Thus, additional factors are likely involved in conveying mating experience to the female's higher brain centers.

A learning circuit underpins mating-induced female preference behavior

Activation of PAM cluster DANs innervating the β'1 region of the MB was sufficient to induce mated female polyamine choice behavior in virgin females, while inhibition of MBON-β'1 output at the time of mating prevented the switch to mated female behavior. Similarly, activation of MBON-β'1 output instead of mating also increased the virgin's polyamine attraction to mated female levels. In addition, MBONs and DANs innervating β'1 respond to the pheromone cVA. We thus propose that mating-induced modulation of the relative activity and output of the β'1 compartment of the MB changes the female's interest in the beneficial compound polyamine. Notably, β'1 MBONs have been implicated previously in courtship conditioning in *Drosophila* males (Montague & Baker, 2016). At this point, we can only speculate about what β'1 MB output does to these reproduction related behaviors. EM connectomics and trans-TANGO data suggest that β'2 DANs are directly and β'2 MBONs indirectly connected to MBON-β'1. In line with this, we find that blocking β'2 MBON output increases the virgin's attraction to polyamine at the time of test.

Like previous work indicating that the expression of associative learning requires the activity of specific LHONs (Dolan et al., 2018), we also find that AD1b2 LHONs are involved in the expression of putrescine attraction in mated females. How a mating-induced modulation of the β'1 compartment is relayed to the LH remains to be further investigated. It is possible that another MBON, MBON-α2sc, which connects from the MB to specific neurons in the LH, is involved (see Fig. S7).

If the mating-induced long-lasting changes in polyamine odor preference are due to a learning mechanism, why do we only see mating-induced changes in β'1-DANs but not in β'1 or β'2 MBONs? One possible explanation could be that the changes are subtle and would require the analysis of a significantly higher number of animals. Alternatively, they could be short-lived and observable only at a very specific time point in these MBONs after mating that we were not fortunate enough to hit in our imaging experiments. It is also conceivable that, as the behavioral data indicates, the role of the β'1 compartment is complex and bidirectional, possibly with subtypes of β'1-innervating DANs that connect to different downstream neurons and receive different inputs (see also Fig. S3E, 6F, S6H,I). Mating could affect these subtypes differently such that a difference is difficult to identify at the current resolution of split-Gal4 lines.

Does reproduction induce neural network changes to facilitate reproductive behaviors?

A state change, such as before and after mating, could conceivably represent a window of opportunity for changes in relevant neural networks (Griffith & Ejima, 2009) or even globally in many or all brain regions. Our *in vivo* whole brain imaging data suggests that, at least in female flies, mating does not induce a global change in brain state. Rather, mating appears to induce discrete changes in a dopamine-gated learning circuit. In line with this interpretation, mating and SPR signaling were recently shown to enhance MB-dependent long-term memory in *Drosophila* females (Scheunemann, Lampin-Saint-Amaux, Schor, & Preat, 2019). Similar scenarios as through mating might arise at times of hunger (Krashes et al., 2009; Root, Ko, Jafari, & Wang, 2011). In other words, food consumed when hungry not only tastes and smells better, it also leaves a longer lasting impression. Mechanistically, such a window of enhanced plasticity might arise through an increase in cAMP in neurons of the MB network at critical phases of life (Louis, Stahl, Boto, & Tomchik, 2018).

Beyond insects, such a scenario could arise during different periods of important changes in the body (Carlson, Gadziola, Dauster, & Wesson, 2018). An example could be mother-child-bonding in mammals where mother and newborn are particularly sensitive to memorizing the sensory characteristics of each other for a certain period after birth (Cernoch & Porter, 1985; Galbally, Lewis, Ijzendoorn, & Permezel, 2011; Sullivan, 2003). For instance, the neuropeptide oxytocin, which is released during birth and lactation, induces lasting changes in the mother's cortex, transforming weaker responses to pup calls in the virgin to strong responses in mothers (Marlin et al., 2015). The orchestration of internal state-dependent sensory tuning with plasticity of neurons in higher brain centers could, thus, ensure that animals remember the most relevant information at key turning points in their lives.

MATERIALS and METHODS

540

KEY RESOURCES TABLE

REAGENT or RESOURCE	SOURCE	IDENTIFIER
Antibodies		
Anti-Mouse Alexa488	Molecular Probes	AB_221544
Anti-Mouse Alexa633	Molecular Probes	AB_141431
Anti-Rabbit Alexa568	Molecular Probes	AB_141416
Anti-Rabbit Alexa633	Molecular Probes	AB_2535731
Anti-Rat Alexa568	Molecular Probes	AB_141874
Mouse monoclonal anti-ChAT	(Yasuyama et al., 1995)	N/A
Mouse monoclonal anti-OA	Jena Bioscience	AB_2315000
Rabbit polyclonal anti-dsRed	Clontech	AB_10013483
Rabbit polyclonal anti-Tyr	Millipore	AB_11215460
Rat monoclonal anti-GFP [3H9]	Chromotek	AB_10773374
Rat monoclonal anti-Ncadherin	DSHB	AB_528121
Data		
All original data is available upon request.		
Experimental Models: Organisms/Strains		
D.mel/Canton-S	Bloomington DSC	Flybase: FBst0064349
D.mel/GMR95A10-LexA	Bloomington DSC	FlyBase: FBst0061633
D.mel/LexAop2-mCD8-GFP	Bloomington DSC	FlyBase: FBst0056182
D.mel/LexAop-P2X2	Bloomington DSC	FlyBase: FBst0076030
D.mel/MB10B	Janelia RC	Flybase: FBst0068293
D.mel/MB11B	Janelia RC	Flybase: FBst0068294
D.mel/MB438B	Janelia RC	Flybase: FBst0068326
D.mel/MB57B	Janelia RC	Flybase: FBst0068277
D.mel/MB60B	Janelia RC	Flybase: FBst0068279
D.mel/MB58B	Janelia RC	FlyBase: FBst0068278
D.mel/MB80C	Janelia RC	FlyBase: FBst0068285
D.mel/MB188B	Janelia RC	gift of Yoshinori Aso
D.mel/MB42B	Janelia RC	FlyBase: FBst0068303
D.mel/MB109B	Janelia RC	gift of Yoshinori Aso
D.mel/MB316B	Janelia RC	gift of Yoshinori Aso
D.mel/L166	Janelia RC	gift of Greg Jefferis
D.mel/L290	Janelia RC	gift of Greg Jefferis
D.mel/L542	Janelia RC	gift of Greg Jefferis
D.mel/L989	Janelia RC	gift of Greg Jefferis
D.mel/L1293	Janelia RC	gift of Greg Jefferis
D.mel/L1479	Janelia RC	gift of Greg Jefferis
D.mel/L1614	Janelia RC	gift of Greg Jefferis
D.mel/L1538	Janelia RC	gift of Greg Jefferis
D.mel/L1539	Janelia RC	gift of Greg Jefferis

D.mel/L1779	Janelia RC	gift of Greg Jefferis
D.mel/L2446	Janelia RC	gift of Greg Jefferis
D.mel/L2382	Janelia RC	gift of Greg Jefferis
D.mel/pBDP-Gal4U (‚empty-Gal4')	Bloomington DSC	Flybase: FBst0068384
D.mel/Tdc2-Gal4	Bloomington DSC	FlyBase: FBst0009313
D.mel/TH-C1-Gal4	(Liu et al., 2012b)	FlyBase: FBtp0083567
D.mel/TH-D1-Gal4	(Liu et al., 2012b)	FlyBase: FBtp0083568
D.mel/TH-F1-Gal4	(Liu et al., 2012b)	FlyBase: FBtp0083570
D.mel/TH-Gal4	Bloomington DSC	FlyBase: FBst0008848
D.mel/UAS-CsChrimson	Bloomington DSC	FlyBase: FBst0055134
D.mel/UAS-DenMark	Bloomington DSC	FlyBase: FBst0033062
D.mel/UAS-GCaMP6f	Bloomington DSC	FlyBase: FBst0042747
D.mel/UAS-mCD8-GFP	Bloomington DSC	FlyBase: FBst0030001
D.mel/UAS-Shibire^{ts1}	Bloomington DSC	FlyBase: FBst0044222
D.mel/UAS-syt-GFP	Bloomington DSC	FlyBase: FBst0006926
D.mel/w1118	Bloomington DSC	Flybase: FBst0003605
D.mel/prd-gal4		gift of Anne von Philipsborn
D.mel/UAS-Bip RNAi		gift of Anne von Philipsborn
D.mel/tud[1] bw[1] sp[1]/CyO, l(2)DTS513[1]	Bloomington DSC	stock # 1786
D.mel/ovoD	Bloomington DSC	stock # 38444
Software and Algorithms		
Matplotlib 1.4.2	(Hunter, 2007)	matplotlib.org
Numpy 1.8	(Travis, 2006)	numpy.org
Prism 6 and 7	GraphPad	graphpad.com/scientific-software/prism
Python 2.7	(van Rossum, 1995)	python.org
Pyvttbl 0.5.2.2	(Lew, 2011)	github.com/rogerlew/pyvttbl
Scipy.stats 0.14	(Jones et al., 2001)	scipy.org
pCLAMP 10.3	Molecular Devices	moleculardevices.com
Igor Pro 6.37	Wave Metrics	wavemetrics.com
NeuroMatic 3.0	(Rothman and Silver, 2018)	neuromatic.thinkrandom.com/
LAS AF E6000 and LAS X	Leica Microsystems	leica-microsystems.com
FV10-ASW	Olympus	olympus-lifescience.com

Fly husbandry

Flies were kept at 25 ℃ at 60 % humidity with a day:night cycle of 12 hours each. Flies were raised on standard cornmeal medium. Mushroom body lines were received from the Janelia Fly-Light Split-GAL4 Driver Collection (Aso, Hattori, et al., 2014). *BiP, prd* lines were a generous gift from Anne von Philipsborn, trans-TANGO lines were a gift from the Barnea Lab, LH lines were kindly provided by Greg Jefferis.

Experiments with wildtype flies

After eclosion, female virgins were kept in a vial until testing one week later. A second group of female flies were kept with males for 24 h. Then, the males were removed, and the females were kept separately in a fresh vial until final testing 3-5 days later. For virgins and mated females, vials were checked for larvae to ensure mating did not or did take place, respectively.
To test the effect of cVA (11-cis-Vaccenyl acetate) exposure on virgin females, 50µl cVA (pure, Pherobank) or as a control ddH_2O were deposited onto a small filter paper disc and added to the food vial containing 1-2 day old virgins. The discs were placed between two layers of mesh to prevent flies from touching or tasting the solution on the disc. After exposure for 24 h, the flies were transferred into a clean vial and tested in a T-maze 3 days later.

Shibire and dTrpA1 experiments

For shibire^{ts1}- and dTrpA1 -silencing or -activation, respectively, flies were shifted to a temperature of 30 ℃ for time frames indicated in the results section.
For temperature shifts *at mating*, 1-2 day old virgin females were put on 30 ℃ for 30 minutes before experienced CantonS males were added for 24 h at 30 ℃ to allow mating during this time period. The males were removed after 24 h. Females were tested 3-5 days later for putrescine preference behavior at 25 ℃ in a T-maze assay. The vials were checked for offspring to ensure mating had taken place. For virgin experiments, virgins were kept for 24 h at 30 ℃ without males. This was followed 3-5 days later for putrescine preference behavior at 25 ℃ in a T-maze assay.
For temperature shifts *at testing*, 1 day old females were kept with males for 24 h at 25 ℃. Then, the males were removed, and females were tested 3-5 days later for putrescine preference behavior. Virgins were not exposed to males. Flies were tested in a preheated T-maze chamber at 30 ℃ and 60 % humidity.

T-maze experiments

The two-choice population assay or T-maze was performed as previously described in (Lewis et al., 2015). T-maze tubes were either prepared with 50 µl of 100 mM 1,4-Diaminobutane (Putrescine, Sigma), 50 µl ultrapure water or different concentrations of ammonia on a piece of Whatman filter paper and sealed with Parafilm until right before the experiment started. Note that the concentration of putrescine is higher than previously reported in Hussain et al. due to a change odor solution preparation as follows. To ensure precise odor concentrations, solid 1,4-Diaminobutane was heated mildly until the solid pieces became liquid. The precise amount was pipetted directly from the solution and diluted in water. Odor solutions were stored at 4 °C for a maximum of 14 days, because of the rapid degradation of putrescine molecules in water and air. Thus, it is important to note that the precise concentration of 1,4-Diaminobutane varied and was usually lower than the initial concentration of 100mM. To ameliorate the problem of fast molecule degradation, odor solution efficacy was regularly tested on CantonS wildtype mated and virgin females and remade if the expected attraction of mated females and low attraction of virgin females was not observed. For the test, flies were tested in groups of ~30 in a non-aspirated T-maze and were allowed 1 min to respond to stimuli. Experimentation was carried out in climate-controlled boxes at 30°C and 60% rH. A preference index (PI) was calculated by subtracting the number of flies on the control side by the number of flies on the stimulus side and normalizing by the total number of flies. The data is represented by bar graphs of the PIs plus standard error of the mean (SEM) and was analyzed using a Mann-Whitney-U test in R-software. This has been done in Excel's RealStats Resource Pack. Unless indicated otherwise, significance stars or n.s. concern the comparison between the two virgin groups or the two mated fly groups, respectively.
Given the importance of reproductive state, we used a single fly assay in order to be able to confirm the

595 reproductive state of each animal tested. All virgin flies that laid fertilized eggs in the days after an experiment were excluded from the analysis. Similarly, all mated females that did not lay fertilized eggs were equally excluded. For single fly T-maze experiments, single mated or virgin females were tested in the same T-maze setup as described above. They were given 1 min to make a choice between water and putrescine. The data is represented as percentage of flies that made a certain choice in bar graphs and was
600 analyzed using a Fisher's exact test in R-software. This has been done in Excel's RealStats Resource Pack. Unless indicated otherwise, significance stars or n.s. concern the comparison between the two virgin groups or the two mated fly groups, respectively.
All experiments were carried out with the experimenter unaware of the genotype or state of the sample. In addition, most experiments were repeated independently by another person in the laboratory.
605

Courtship experiments

Male flies were kept together in a vial for 2 days until exposure to 1-2 days old virgin females. Always one male was put into a vial with one female. The process of courtship as described in previous studies (Dickson, 2008) was monitored until the male began licking the female and making first attempts for
610 copulation. Immediately, the male was removed from the vial. The female was tested 3-5 days later in a T-maze for putrescine attraction or avoidance behavior at 25 ℃.

Immunohistochemistry

Trans-TANGO flies were kept for one week at 25 ℃ followed by another two weeks at 18 ℃, as similarly
615 described in the original paper (Talay et al., 2017). Flies were anaesthetized on ice, put in a glass staining cup with 80 % ethanol. After 30 sec flies were put in another glass staining cup filled with 1x phosphate buffered saline (PBS). Flies were dissected under the microscope and brains were stored in a PCR cap with 1:4 solution of 4 % paraformaldehyde (PFA) and 0.1 % phosphate buffered triton (PBT) until final fixation. Brains were fixed in PFA and a drop of PBT for 60 min at room temperature. Brains were then washed with
620 PBT three times for 20 min at room temperature. The PBT was removed and replaced by 3 % normal goat serum (NGS) for 30 min at room temperature. The first antibody mix was incubated in 1:200 with α-GFP (mouse), α-RFP (rabbit), α-NCAD (rat)and 3 % NGS for 24 h at 4 ℃ in darkness. Brains were washed with PBT for 5 sec and then three times for 20 min at 4 ℃ in darkness. The second antibody mix was incubated at 1:200 with α-mouse alexa488, α-rabbit Cy3, α-rat alexa633 and 3 % NGS for 24 h at 4 ℃ in darkness.
625 Brains were washed with PBT for 5 sec and then three times for 20 min at 4 ℃ in darkness. After washing with PBT for one last time for 1 h at 4 ℃ in darkness, brains were mounted on a glass slide with VectaShield. Imaging was carried out at a Leica SP8 confocal microscope. Image Processing and analysis have been performed using Fiji software (Schindelin et al., 2012).

630 **Electron microscopy connectomics**

All images, connectomes and related data were obtained by working with the database NeuPrint (https://neuprint.janelia.org). Connectomes and reconstructed images only depict subsets of neurons and not all neurons that are synaptically connected to each other.

635 ***In vivo* 2-Photon calcium imaging**

All imaging experiments were conducted with a two-photon microscope. 5- to 7-day-old female virgin or mated flies of the genotype MB188B-Gal4;UAS-GCaMP6f for PAM neuron imaging and MB057B-Gal4; UAS-GCaMP6f for MBON imaging were used. *In vivo* fly preparations were prepared according to a

method described previously. Preparations were imaged using an Olympus FV1000 two-photon microscope
640 system with a BX61WI microscope and a 40 x , 0.8 water immersion objective. GCaMP fluorescence was excited at 910 nm by a mode-locked Ti:Sapphire Mai Tai DeepSee laser. Time series images were acquired at 256 x 256 pixel resolution at a rate of 2 frames per second for 40 frames using the Olympus FV10-ASW imaging software. In order to minimize the brain movement of *in vivo* preparations under the two-photon microscope, a drop of 1% low melting temperature agarose (NuSieveGTG, Lonza) in imaging buffer
645 maintained at 37ºC was added to the exposed brain. A custom-made odor delivery system with mass flow controllers was used for vinegar stimulation. The odor was delivered in a continuous airstream (1000 mL/min) through a 8-mm Teflon tube placed ~1 cm away from the fly. *In vivo* two-photon time series data were acquired at a rate of ~4 frames/s with 175 x 175 pixel resolution. Changes in fluorescence intensity were measured in manually drawn regions of interest (ROI) using the LAS AF E6000 Lite, LAS X or the
650 Olympus FV10-ASW software. Relative changes in fluorescence intensity were defined as $\Delta F/F = 100^* (F_i - F_0)/F_0$ for the i frames after stimulation. Fluorescence background, F_0, is the average fluorescence of 60 frames (1 min; *ex vivo*), 5 frames (~1 s; *in vivo*, two-photon), 20 frames (~1 s; *in vivo*, ATP static) or 17 frames (~1 s; *in vivo*, ATP perfused). Pseudocolored images were generated using a custom-written MATLAB program and ImageJ.
655

***In vivo* light field calcium imaging**

Female flies (*nsyb-Gal4;UAS-Gcamp6s*) were collected at eclosion to obtain virgins or mated for 48 h with males of the same genotype. After the males were removed from the mated group, the labels of both groups were blinded to avoid bias. Successful mating or virginity was confirmed later by keeping the vials at 25°C
660 and checking for larvae a few days after the experiment. Flies were prepared for whole brain imaging at Day 4 after eclosion, as previously described (Woller et al., 2021). The light field microscope was set up according to (Aimon et al., 2019). The system was based on a Thorlabs Cerna with a Leica HC FLUOTAR L 25x/0.95 objective and MLA-S125-f12 microlens array (RPC photonics). The microlens array was placed on the image plane, while the camera imaged the microlens array through 50mmf/1.4 NIKKOR-S Nikon
665 relay lenses. The light field images were recorded at 10 Hz with a scientific CMOS camera (Hamamatsu ORCA-Flash 4.0). For odor delivery, a Syntech Stimulus Controller (CSS-55) was connected to a 4 mm PVC tube that was placed under the microscope, 5 mm in front of the fly's head and delivered a constant air stream of 1000 ml/min. Flies were stimulated by redirecting 30% of main air flow for 1 sec through a head-space glass vial filled with 1 ml of 100mM putrescine by a manual trigger. Each fly was stimulated five
670 times with 50 sec interstimulus intervals. The imaging data was processed as described in (Siju et al., 2020). Volumes were reconstructed using a python program developed by Broxton et al. (2013) (Broxton et al., 2013) and available on github: https://github.com/sophie63/FlyLFM. The movement artifacts were removed by 3D registration using the 3dvolreg routine from AFNI. The following steps were performed with MATLAB (version R2019b, MathWorks Inc.) unless stated otherwise. The voxel time series were
675 transformed to DF/F by subtracting and normalizing by a moving average over 20 s and noise was reduced, using Kalman filtering. Functional regions were then extracted using principal component analysis and independent component analysis. These were then used as landmarks to align the recordings to anatomical templates from (**Ito** et al., 2014) in FIJI. Masks were created to extract and average DF/F time series for twelve major brain regions (neuropil supercategories). Linear regression of the response time series with the
680 stimulus time series (convolved with the response profile of GCamp6s) was performed. Peak responses to the first four odor stimulations were calculated by subtracting the mean DF/F in a 5 sec window before the stimulus from the maximum value in the 20 sec window after the stimulus. Interstimulus phases were extracted as 30 sec intervals (10 seconds after a stimulus and 10 seconds before the next stimulus).

Statistical analysis was performed with GraphPad Prism (version 9.1.2, GraphPad Software LLC).

Chemical analysis of fly food

Chemicals

The following compounds were obtained commercially from the sources given in parentheses: formic acid, sodium hydroxide (Merck, Darmstadt, Germany), histamine, ethanolamine, 2-phenylethylamine, putrescine, β-alanine, tyramine, spermine, spermidine, trichloroacetic acid (Sigma-Aldrich, Taufkirchen, Germany), benzoyl chloride (VWR, Darmstadt, Germany), [2H4]-histamine, [2H4]-putrescine (CDN Isotopes, Quebec, Canada), [13C2]-ethanolamine, [13C3,15N]-β-alanine (Sigma-Aldrich, St. Louis, MO, USA), [2H4]-phenylethylamine (Dr. Ehrenstorfer, Augsburg, Germany). The purity of all amines was checked by LC-MS and NMR experiments as described by Mayr and Schieberle (Mayr & Schieberle, 2012). Deuterated solvents were obtained from Euriso-Top (Gif-Sur-Yvette, France). Solvents used for HPLC-MS/MS analysis were of LC-MS grade (Honeywell, Seelze, Germany); all other solvents were of HPLC grade (Merck Darmstadt, Germany). Water used for HPLC separation was purified by means of a Milli-Q water advantage A 10 water system (Millipore, Molsheim, France). [2H4]-Spermine, [2H2]-tyramine and [2H4]-spermidine were synthesized and purified as reported earlier (Mayr & Schieberle, 2012). Standard flyfood consisted of the following ingredients: agar, corn flour, soy flour, yeast, malt, molasses, nipagin, ethanol, phosphoric acid.

Analysis of amines in fly food samples

Quantification of biogenic amines and polyamines in flyfood was performed by means of a stable isotope dilution LC-MS/MS method after derivatization as already reported by Mayr and Schieberle (Mayr & Schieberle, 2012). Stock solutions. Stock solutions of the internal standards [13C3]-ethanolamine (52 µg/mL), [13C3,15N]-β-alanine (36.0 µg/mL), [2H4]-histamine (66.87 µg/mL), [2H4]-putrescine (28.86 µg/mL), [2H4]-spermine (91.56 µg/mL), [2H2]-tyramine (51 µg/mL) and [2H4]-spermidine (230 µg/mL) and [2H4]-phenylethylamine (109 µg/mL) were prepared in aqueous tri-chloro-acetic acid (10 %) and stored at 7 ℃ until use.

Sample workup

Flyfood was frozen in liquid nitrogen and grounded in a mill (Moulinette, Moulinex, France). Aliquots (5 g) of each sample were spiked with an aliquot of the labled internal standards ([13C3, 15N]β-alanine 50 µL, [2H4]-histamine 100 µL, [2H4]-putrescine 100 µL, [2H4]-spermine 50 µL, [2H2]-tyramine 100 µL, [2H4]-spermidine 50 µL, and [2H4]-phenyl-ethylamine 109 µL), thereafter, aqueous tri-chloro-acetic acid (10 %, 40 mL) was added, and vigorously stirred at room temperature. After an equilibration time of 30 min, the suspension was homogenated using an Ultraturrax (3 min, Jahnke and Kunkel, IKA-Labortechnik, Staufen im Breisgau, Germany), and ultrasonificated for another 10 minutes. The suspension obtained was centrifuged (10 min, 8000 rpm) and, finally, filtered (Schleicher & Schuell filter). The pH of the filtrate was adjusted to 10 with aqueous sodium hydroxide (1 M) and a solution of benzoyl chloride dissolved in acetonitrile (30 mL; 1 g/250 mL ACN) was added. After stirring for 2 h at room temperature pH was adjusted to pH 2-3 using HCl (conc.). The benzamides were then extracted with dichloromethane (3 x 20 mL), and the organic phases were combined, dried over Na_2SO_4, and evaporated to dryness at 30 ℃. The residue was dissolved in a mixture of acetonitrile and 0.1 % aqueous formic acid (20/80, v/v) and filtered over a syringe filter (0.45 µm; Spartan 13/0.45 RC; Schleicher and Schuell, Dassel, Germany). The final filtrate was diluted with water (1/20, v/v). An aliquot (10 µL) of the prepared sample was injected into the HPLC-MS/MS system.

High Performance Liquid Chromatography-Triple Quadrupole Mass Spectrometry (HPLC-MS/MS). HPLC-

MS/MS analysis was performed on a Surveyor high-performance chromatography system (Thermo Finnigan, Dreieich, Germany), equipped with a thermostated autosampler and a triple-quadrupol tandem mass spectrometer TQS Quantum Discovery (Thermo Electron, Dreieich, Germany). Temperature of the column compartment was set at 30 ℃ and autosampler temperature was 24 ℃. After sample injection (10 µL), chromatography was carried out on a Synergy Fusion RP \SI 80 Å column (150 x 2.0 mm id, 4 µm, Phenomenex, Aschaffenburg, Germany) using the following solvent gradient (0.2 mL/min) of acetonitrile (0.1 % formic acid) as solvent A and formic acid (0.1 % in water) as solvent B: 0 min, 0 % A; 1 min, 0 % A; 1.5 min, 35 % A; 20 min, 40 % A; 26 min, 50 % A; 27 min, 90 % A; 36 min, 90 % A; 37 min, 0 % A.; 52 min, 0 % A. The mass spectrometer was operated in the positive electrospray ionization (ESI+) mode, the spray needle voltage was set at 3.5 kV, the spray current at 5 µA, the temperature of the capillary was 300, the capillary voltage at 35 V. Nitrogen served as sheath and auxiliary gas, which was adjusted to 40 and 10 arbitary units. The collision cell was operated at a collision gas (argon) pressure of 0.13 Pa. Mass transitions of the pseudo molecular ions ([M+H]+) into specific product ions are summarized in Mayr and Schieberle (Mayr & Schieberle, 2012). Calibration curves for the calculation of the response factors and linear ranges of the analytes were measured as described before by Mayr and Schieberle (Mayr & Schieberle, 2012).

Acknowledgments

We thank our project students C. Biermeier, A. Erb, D. Mostert, V. Statovskii, K. Wald, R. Raab and D. Zapoglou for cross-validating T-maze experiments in independent experiments in single and multi-fly assays and extended research support for this project. We wish to acknowledge S. Aimon for helping us with whole brain imaging and imaging data analysis. We would especially like to thank Heidi Miller-Mommerskamp for technical support. Thanks also to A. Bates, M. Costa and G. Jefferis for discussions regarding neurons of the lateral horn and access to EM tracing data. We acknowledge the Barnea, Jefferis and von Philipsborn labs for the provided fly lines. We are grateful to D. Neumeier and S. Kaviani-Nejad for technical assistance regarding the work on the polyamine concentration analysis in food. We would also like to thank N. Gompel, S. Sachse, K. Vogt and members of the Grunwald Kadow laboratory for comments on the manuscript and valuable feedback. This work was supported by the European Union (H2020, ERC starting grant 'FlyContext' to IGK) and the German research foundation (SFB870, A04 to IGK, and GR4310/5-1).

Author Contributions

AB and IGK wrote the manuscript with help of all other authors. AB and IGK designed the study. AB conducted most of the single-fly experiments. JC conducted the MBON experiments at testing with Shibire^{ts1}. MHL conducted the dTrpA1 at testing experiments, AB trained JC and MHL and cross-validated the experiments. AF and SH screened all lateral horn lines and cross-validated several mushroom body line and additional experiments using T-maze assays. AF and AB carried out the immunohistochemistry experiments. AF performed all confocal imaging. SKP performed multiphoton calcium imaging experiments. PB performed and analyzed the whole brain lightfield imaging experiments. CD and TH provided the analysis of polyamine concentration in our fly food. All authors approved to the final version of the manuscript.

Declaration of Interests

The authors declare no competing interests.

References

775 Aimon, S., Cheng, K. Y., Gjorgjieva, J., & Grunwald Kadow, I. C. (2022). Walking elicits global brain activity in Drosophila. *bioRxiv*, 2022.2001.2017.476660. doi:10.1101/2022.01.17.476660

Aimon, S., Katsuki, T., Jia, T., Grosenick, L., Broxton, M., Deisseroth, K., . . . Greenspan, R. J. (2019). Fast near-whole-brain imaging in adult Drosophila during responses to stimuli and behavior. *PLoS Biol, 17*(2), e2006732. doi:10.1371/journal.pbio.2006732

780 Aso, Y., Hattori, D., Yu, Y., Johnston, R. M., Iyer, N. A., Ngo, T. T., . . . Rubin, G. M. (2014). The neuronal architecture of the mushroom body provides a logic for associative learning. *Elife, 3*, e04577. doi:10.7554/eLife.04577

Aso, Y., Sitaraman, D., Ichinose, T., Kaun, K. R., Vogt, K., Belliart-Guerin, G., . . . Rubin, G. M. (2014). Mushroom body output neurons encode valence and guide memory-based action selection in
785 Drosophila. *Elife, 3*, e04580. doi:10.7554/eLife.04580

Azanchi, R., Kaun, K. R., & Heberlein, U. (2013). Competing dopamine neurons drive oviposition choice for ethanol in Drosophila. *Proc Natl Acad Sci U S A, 110*(52), 21153-21158. doi:10.1073/pnas.1320208110

Boswell, R. E., & Mahowald, A. P. (1985). tudor, a gene required for assembly of the germ plasm in
790 Drosophila melanogaster. *Cell, 43*(1), 97-104. doi:10.1016/0092-8674(85)90015-7

Bracker, L. B., Siju, K. P., Varela, N., Aso, Y., Zhang, M., Hein, I., . . . Grunwald Kadow, I. C. (2013). Essential role of the mushroom body in context-dependent CO(2) avoidance in Drosophila. *Curr Biol, 23*(13), 1228-1234. doi:10.1016/j.cub.2013.05.029

Broxton, M., Grosenick, L., Yang, S., Cohen, N., Andalman, A., Deisseroth, K., & Levoy, M. (2013). Wave
795 optics theory and 3-D deconvolution for the light field microscope. *Opt Express, 21*(21), 25418-25439. doi:10.1364/OE.21.025418

Carlson, K. S., Gadziola, M. A., Dauster, E. S., & Wesson, D. W. (2018). Selective Attention Controls Olfactory Decisions and the Neural Encoding of Odors. *Curr Biol, 28*(14), 2195-2205 e2194. doi:10.1016/j.cub.2018.05.011

800 Carnell, S., Gibson, C., Benson, L., Ochner, C. N., & Geliebter, A. (2012). Neuroimaging and obesity: current knowledge and future directions. *Obes Rev, 13*(1), 43-56. doi:10.1111/j.1467-789X.2011.00927.x

Cernoch, J. M., & Porter, R. H. (1985). Recognition of maternal axillary odors by infants. *Child Dev, 56*(6), 1593-1598. Retrieved from http://www.ncbi.nlm.nih.gov/pubmed/4075877

Chapman, T., Bangham, J., Vinti, G., Seifried, B., Lung, O., Wolfner, M. F., . . . Partridge, L. (2003). The sex
805 peptide of Drosophila melanogaster: female post-mating responses analyzed by using RNA interference. *Proc Natl Acad Sci U S A, 100*(17), 9923-9928. doi:10.1073/pnas.1631635100

Chapman, T., & Wolfner, M. F. (2017). Reproductive behaviour: Make love, then war. *Nat Ecol Evol, 1*(6), 174. doi:10.1038/s41559-017-0174

Chin, S. G., Maguire, S. E., Huoviala, P., Jefferis, G., & Potter, C. J. (2018). Olfactory Neurons and Brain
810 Centers Directing Oviposition Decisions in Drosophila. *Cell Rep, 24*(6), 1667-1678. doi:10.1016/j.celrep.2018.07.018

Chow, C. Y., Avila, F. W., Clark, A. G., & Wolfner, M. F. (2015). Induction of excessive endoplasmic reticulum stress in the Drosophila male accessory gland results in infertility. *PLoS One, 10*(3), e0119386. doi:10.1371/journal.pone.0119386

815 Chu, B., Chui, V., Mann, K., & Gordon, M. D. (2014). Presynaptic gain control drives sweet and bitter taste integration in Drosophila. *Curr Biol, 24*(17), 1978-1984. doi:10.1016/j.cub.2014.07.020

Cohn, R., Morantte, I., & Ruta, V. (2015). Coordinated and Compartmentalized Neuromodulation Shapes Sensory Processing in Drosophila. *Cell, 163*(7), 1742-1755. doi:10.1016/j.cell.2015.11.019

Cury, K. M., Prud'homme, B., & Gompel, N. (2019). A short guide to insect oviposition: when, where and
820 how to lay an egg. *J Neurogenet, 33*(2), 75-89. doi:10.1080/01677063.2019.1586898

Das, S., Trona, F., Khallaf, M. A., Schuh, E., Knaden, M., Hansson, B. S., & Sachse, S. (2017). Electrical synapses mediate synergism between pheromone and food odors in Drosophila melanogaster. *Proc Natl Acad Sci U S A, 114*(46), E9962-E9971. doi:10.1073/pnas.1712706114

Dey, S., Chamero, P., Pru, J. K., Chien, M. S., Ibarra-Soria, X., Spencer, K. R., . . . Stowers, L. (2015). Cyclic
825 Regulation of Sensory Perception by a Female Hormone Alters Behavior. *Cell, 161*(6), 1334-1344.

doi:10.1016/j.cell.2015.04.052
Dickson, B. J. (2008). Wired for sex: the neurobiology of Drosophila mating decisions. *Science, 322*(5903), 904-909. doi:322/5903/904 [pii]
10.1126/science.1159276
Dolan, M. J., Belliart-Guerin, G., Bates, A. S., Frechter, S., Lampin-Saint-Amaux, A., Aso, Y., . . . Jefferis, G. (2018). Communication from Learned to Innate Olfactory Processing Centers Is Required for Memory Retrieval in Drosophila. *Neuron, 100*(3), 651-668 e658. doi:10.1016/j.neuron.2018.08.037
Dolan, M. J., Frechter, S., Bates, A. S., Dan, C., Huoviala, P., Roberts, R. J., . . . Jefferis, G. S. (2019). Neurogenetic dissection of the Drosophila lateral horn reveals major outputs, diverse behavioural functions, and interactions with the mushroom body. *Elife, 8*. doi:10.7554/eLife.43079
Ebrahim, S. A., Dweck, H. K., Stokl, J., Hofferberth, J. E., Trona, F., Weniger, K., . . . Knaden, M. (2015). Drosophila Avoids Parasitoids by Sensing Their Semiochemicals via a Dedicated Olfactory Circuit. *PLoS Biol, 13*(12), e1002318. doi:10.1371/journal.pbio.1002318
Ejima, A., Smith, B. P., Lucas, C., van der Goes van Naters, W., Miller, C. J., Carlson, J. R., . . . Griffith, L. C. (2007). Generalization of courtship learning in Drosophila is mediated by cis-vaccenyl acetate. *Curr Biol, 17*(7), 599-605. doi:10.1016/j.cub.2007.01.053
Frechter, S., Bates, A. S., Tootoonian, S., Dolan, M. J., Manton, J. D., Jamasb, A. R., . . . Jefferis, G. S. (2019). Functional and anatomical specificity in a higher olfactory centre. *Elife, 8*. doi:10.7554/eLife.44590
Galbally, M., Lewis, A. J., Ijzendoorn, M., & Permezel, M. (2011). The role of oxytocin in mother-infant relations: a systematic review of human studies. *Harv Rev Psychiatry, 19*(1), 1-14. doi:10.3109/10673229.2011.549771
Gou, B., Liu, Y., Guntur, A. R., Stern, U., & Yang, C. H. (2014). Mechanosensitive neurons on the internal reproductive tract contribute to egg-laying-induced acetic acid attraction in Drosophila. *Cell Rep, 9*(2), 522-530. doi:10.1016/j.celrep.2014.09.033
Griffith, L. C., & Ejima, A. (2009). Courtship learning in Drosophila melanogaster: diverse plasticity of a reproductive behavior. *Learn Mem, 16*(12), 743-750. doi:16/12/743 [pii]
10.1101/lm.956309
Grosjean, Y., Rytz, R., Farine, J. P., Abuin, L., Cortot, J., Jefferis, G. S., & Benton, R. (2011). An olfactory receptor for food-derived odours promotes male courtship in Drosophila. *Nature, 478*(7368), 236-240. doi:10.1038/nature10428
Grunwald Kadow, I. C. (2018). State-dependent plasticity of innate behavior in fruit flies. *Curr Opin Neurobiol, 54*, 60-65. doi:10.1016/j.conb.2018.08.014
Hadjieconomou, D., King, G., Gaspar, P., Mineo, A., Blackie, L., Ameku, T., . . . Miguel-Aliaga, I. (2020). Enteric neurons increase maternal food intake during reproduction. *Nature, 587*(7834), 455-459. doi:10.1038/s41586-020-2866-8
Handler, A., Graham, T. G. W., Cohn, R., Morantte, I., Siliciano, A. F., Zeng, J., . . . Ruta, V. (2019). Distinct Dopamine Receptor Pathways Underlie the Temporal Sensitivity of Associative Learning. *Cell, 178*(1), 60-75 e19. doi:10.1016/j.cell.2019.05.040
Heisenberg, M. (2003). Mushroom body memoir: from maps to models. *Nat Rev Neurosci, 4*(4), 266-275. doi:10.1038/nrn1074
nrn1074 [pii]
Hige, T., Aso, Y., Rubin, G. M., & Turner, G. C. (2015). Plasticity-driven individualization of olfactory coding in mushroom body output neurons. *Nature, 526*(7572), 258-262. doi:10.1038/nature15396
Hoekzema, E., Barba-Muller, E., Pozzobon, C., Picado, M., Lucco, F., Garcia-Garcia, D., . . . Vilarroya, O. (2017). Pregnancy leads to long-lasting changes in human brain structure. *Nat Neurosci, 20*(2), 287-296. doi:10.1038/nn.4458
Hussain, A., Ucpunar, H. K., Zhang, M., Loschek, L. F., & Grunwald Kadow, I. C. (2016). Neuropeptides Modulate Female Chemosensory Processing upon Mating in Drosophila. *PLoS Biol, 14*(5), e1002455. doi:10.1371/journal.pbio.1002455
Hussain, A., Zhang, M., Ucpunar, H. K., Svensson, T., Quillery, E., Gompel, N., . . . Grunwald Kadow, I. C. (2016). Ionotropic Chemosensory Receptors Mediate the Taste and Smell of Polyamines. *PLoS Biol, 14*(5), e1002454. doi:10.1371/journal.pbio.1002454

Insel, T. R., Preston, S., & Winslow, J. T. (1995). Mating in the monogamous male: behavioral consequences. *Physiol Behav, 57*(4), 615-627. Retrieved from https://www.ncbi.nlm.nih.gov/pubmed/7777594

Ito, K., Shinomiya, K., Ito, M., Armstrong, J. D., Boyan, G., Hartenstein, V., . . . Insect Brain Name Working, G. (2014). A systematic nomenclature for the insect brain. *Neuron, 81*(4), 755-765. doi:10.1016/j.neuron.2013.12.017

Jeanne, J. M., Fisek, M., & Wilson, R. I. (2018). The Organization of Projections from Olfactory Glomeruli onto Higher-Order Neurons. *Neuron, 98*(6), 1198-1213 e1196. doi:10.1016/j.neuron.2018.05.011

Jefferis, G. S., Potter, C. J., Chan, A. M., Marin, E. C., Rohlfing, T., Maurer, C. R., Jr., & Luo, L. (2007). Comprehensive maps of Drosophila higher olfactory centers: spatially segregated fruit and pheromone representation. *Cell, 128*(6), 1187-1203. doi:S0092-8674(07)00204-8 [pii] 10.1016/j.cell.2007.01.040

Kalac, P. (2014). Health effects and occurrence of dietary polyamines: a review for the period 2005-mid 2013. *Food Chem, 161*, 27-39. doi:10.1016/j.foodchem.2014.03.102

Keleman, K., Vrontou, E., Kruttner, S., Yu, J. Y., Kurtovic-Kozaric, A., & Dickson, B. J. (2012). Dopamine neurons modulate pheromone responses in Drosophila courtship learning. *Nature, 489*(7414), 145-149. doi:10.1038/nature11345

Kim, Y. J., Bartalska, K., Audsley, N., Yamanaka, N., Yapici, N., Lee, J. Y., . . . Dickson, B. J. (2010). MIPs are ancestral ligands for the sex peptide receptor. *Proc Natl Acad Sci U S A, 107*(14), 6520-6525. doi:10.1073/pnas.0914764107

Kitamoto, T. (2001). Conditional modification of behavior in Drosophila by targeted expression of a temperature-sensitive shibire allele in defined neurons. *J Neurobiol, 47*(2), 81-92. doi:10.1002/neu.1018 [pii]

Koch, M., & Ehret, G. (1989). Estradiol and parental experience, but not prolactin are necessary for ultrasound recognition and pup-retrieving in the mouse. *Physiol Behav, 45*(4), 771-776. Retrieved from https://www.ncbi.nlm.nih.gov/pubmed/2780846

Kohl, J., Ostrovsky, A. D., Frechter, S., & Jefferis, G. S. (2013). A bidirectional circuit switch reroutes pheromone signals in male and female brains. *Cell, 155*(7), 1610-1623. doi:10.1016/j.cell.2013.11.025

Krashes, M. J., DasGupta, S., Vreede, A., White, B., Armstrong, J. D., & Waddell, S. (2009). A neural circuit mechanism integrating motivational state with memory expression in Drosophila. *Cell, 139*(2), 416-427. doi:10.1016/j.cell.2009.08.035

Kubli, E. (2003). Sex-peptides: seminal peptides of the Drosophila male. *Cell Mol Life Sci, 60*(8), 1689-1704. doi:10.1007/s00018-003-3052

Lebreton, S., Grabe, V., Omondi, A. B., Ignell, R., Becher, P. G., Hansson, B. S., . . . Witzgall, P. (2014). Love makes smell blind: mating suppresses pheromone attraction in Drosophila females via Or65a olfactory neurons. *Sci Rep, 4*, 7119. doi:10.1038/srep07119

Lebreton, S., Trona, F., Borrero-Echeverry, F., Bilz, F., Grabe, V., Becher, P. G., . . . Witzgall, P. (2015). Feeding regulates sex pheromone attraction and courtship in Drosophila females. *Sci Rep, 5*, 13132. doi:10.1038/srep13132

LeDue, E. E., Mann, K., Koch, E., Chu, B., Dakin, R., & Gordon, M. D. (2016). Starvation-Induced Depotentiation of Bitter Taste in Drosophila. *Curr Biol, 26*(21), 2854-2861. doi:10.1016/j.cub.2016.08.028

Leinwand, S. G., & Chalasani, S. H. (2011). Olfactory networks: from sensation to perception. *Curr Opin Genet Dev, 21*(6), 806-811. doi:10.1016/j.gde.2011.07.006

Leinwand, S. G., & Scott, K. (2021). Juvenile hormone drives the maturation of spontaneous mushroom body neural activity and learned behavior. *Neuron, 109*(11), 1836-1847 e1835. doi:10.1016/j.neuron.2021.04.006

Lewis, L. P., Siju, K. P., Aso, Y., Friedrich, A. B., Bulteel, A. J., Rubin, G. M., & Grunwald Kadow, I. C. (2015). A Higher Brain Circuit for Immediate Integration of Conflicting Sensory Information in Drosophila. *Curr Biol, 25*(17), 2203-2214. doi:10.1016/j.cub.2015.07.015

Li, F., Lindsey, J., Marin, E. C., Otto, N., Dreher, M., Dempsey, G., . . . Rubin, G. M. (2020). The connectome of the adult Drosophila mushroom body: implications for function. *bioRxiv*,

2020.2008.2029.273276. doi:10.1101/2020.08.29.273276
Lin, C. C., Prokop-Prigge, K. A., Preti, G., & Potter, C. J. (2015). Food odors trigger Drosophila males to deposit a pheromone that guides aggregation and female oviposition decisions. *Elife, 4*. doi:10.7554/eLife.08688
Louis, T., Stahl, A., Boto, T., & Tomchik, S. M. (2018). Cyclic AMP-dependent plasticity underlies rapid changes in odor coding associated with reward learning. *Proc Natl Acad Sci U S A, 115*(3), E448-E457. doi:10.1073/pnas.1709037115
Marlin, B. J., Mitre, M., D'Amour J, A., Chao, M. V., & Froemke, R. C. (2015). Oxytocin enables maternal behaviour by balancing cortical inhibition. *Nature, 520*(7548), 499-504. doi:10.1038/nature14402
Mayr, C. M., & Schieberle, P. (2012). Development of stable isotope dilution assays for the simultaneous quantitation of biogenic amines and polyamines in foods by LC-MS/MS. *J Agric Food Chem, 60*(12), 3026-3032. doi:10.1021/jf204900v
Miller-Fleming, L., Olin-Sandoval, V., Campbell, K., & Ralser, M. (2015). Remaining Mysteries of Molecular Biology: The Role of Polyamines in the Cell. *J Mol Biol, 427*(21), 3389-3406. doi:10.1016/j.jmb.2015.06.020
Min, S., Ai, M., Shin, S. A., & Suh, G. S. (2013). Dedicated olfactory neurons mediating attraction behavior to ammonia and amines in Drosophila. *Proc Natl Acad Sci U S A, 110*(14), E1321-1329. doi:10.1073/pnas.1215680110
Montague, S. A., & Baker, B. S. (2016). Memory Elicited by Courtship Conditioning Requires Mushroom Body Neuronal Subsets Similar to Those Utilized in Appetitive Memory. *PLoS One, 11*(10), e0164516. doi:10.1371/journal.pone.0164516
Moshitzky, P., Fleischmann, I., Chaimov, N., Saudan, P., Klauser, S., Kubli, E., & Applebaum, S. W. (1996). Sex-peptide activates juvenile hormone biosynthesis in the Drosophila melanogaster corpus allatum. *Arch Insect Biochem Physiol, 32*(3-4), 363-374. doi:10.1002/(SICI)1520-6327(1996)32:3/4<363::AID-ARCH9>3.0.CO;2-T
Ochsenbein-Kolble, N., von Mering, R., Zimmermann, R., & Hummel, T. (2007). Changes in olfactory function in pregnancy and postpartum. *Int J Gynaecol Obstet, 97*(1), 10-14. doi:10.1016/j.ijgo.2006.12.009
Owald, D., Felsenberg, J., Talbot, C. B., Das, G., Perisse, E., Huetteroth, W., & Waddell, S. (2015). Activity of defined mushroom body output neurons underlies learned olfactory behavior in Drosophila. *Neuron, 86*(2), 417-427. doi:10.1016/j.neuron.2015.03.025
Owald, D., & Waddell, S. (2015). Olfactory learning skews mushroom body output pathways to steer behavioral choice in Drosophila. *Curr Opin Neurobiol, 35*, 178-184. doi:10.1016/j.conb.2015.10.002
Palouzier-Paulignan, B., Lacroix, M. C., Aime, P., Baly, C., Caillol, M., Congar, P., . . . Fadool, D. A. (2012). Olfaction under metabolic influences. *Chem Senses, 37*(9), 769-797. doi:10.1093/chemse/bjs059
Piper, M. D., Blanc, E., Leitão-Gonçalves, R., Yang, M., He, X., Linford, N. J., . . . Partridge, L. (2014). A holidic medium for Drosophila melanogaster. *Nat Methods, 11*(1), 100-105. doi:10.1038/nmeth.2731
Reisenman, C. E., Riffell, J. A., & Hildebrand, J. G. (2009). Neuroethology of oviposition behavior in the moth Manduca sexta. *Ann N Y Acad Sci, 1170*, 462-467. doi:10.1111/j.1749-6632.2009.03875.x
Ribeiro, C., & Dickson, B. J. (2010). Sex peptide receptor and neuronal TOR/S6K signaling modulate nutrient balancing in Drosophila. *Curr Biol, 20*(11), 1000-1005. doi:10.1016/j.cub.2010.03.061
Rolls, E. T. (2007). Sensory processing in the brain related to the control of food intake. *Proc Nutr Soc, 66*(1), 96-112. doi:10.1017/S0029665107005332
Root, C. M., Ko, K. I., Jafari, A., & Wang, J. W. (2011). Presynaptic facilitation by neuropeptide signaling mediates odor-driven food search. *Cell, 145*(1), 133-144. doi:S0092-8674(11)00122-X [pii] 10.1016/j.cell.2011.02.008
Ruta, V., Datta, S. R., Vasconcelos, M. L., Freeland, J., Looger, L. L., & Axel, R. (2010). A dimorphic pheromone circuit in Drosophila from sensory input to descending output. *Nature, 468*(7324), 686-690. doi:10.1038/nature09554
Sayin, S., Boehm, A. C., Kobler, J. M., De Backer, J. F., & Grunwald Kadow, I. C. (2018). Internal State Dependent Odor Processing and Perception-The Role of Neuromodulation in the Fly Olfactory System. *Front Cell Neurosci, 12*, 11. doi:10.3389/fncel.2018.00011

Scheffer, L. K., Xu, C. S., Januszewski, M., Lu, Z., Takemura, S. Y., Hayworth, K. J., . . . Plaza, S. M. (2020). A connectome and analysis of the adult. *Elife, 9*. doi:10.7554/eLife.57443

Scheunemann, L., Lampin-Saint-Amaux, A., Schor, J., & Preat, T. (2019). A sperm peptide enhances long-term memory in female Drosophila. *Sci Adv, 5*(11), eaax3432. doi:10.1126/sciadv.aax3432

Schindelin, J., Arganda-Carreras, I., Frise, E., Kaynig, V., Longair, M., Pietzsch, T., . . . Cardona, A. (2012). Fiji: an open-source platform for biological-image analysis. *Nat Methods, 9*(7), 676-682. doi:10.1038/nmeth.2019

Shao, L., Chung, P., Wong, A., Siwanowicz, I., Kent, C. F., Long, X., & Heberlein, U. (2019). A Neural Circuit Encoding the Experience of Copulation in Female Drosophila. *Neuron, 102*(5), 1025-1036 e1026. doi:10.1016/j.neuron.2019.04.009

Siegel, R. W., & Hall, J. C. (1979). Conditioned responses in courtship behavior of normal and mutant Drosophila. *Proc Natl Acad Sci U S A, 76*(7), 3430-3434. doi:10.1073/pnas.76.7.3430

Siju, K. P., Štih, V., Aimon, S., Gjorgjieva, J., Portugues, R., & Grunwald Kadow, I. C. (2020). Valence and State-Dependent Population Coding in Dopaminergic Neurons in the Fly Mushroom Body. *Curr Biol, 30*(11), 2104-2115.e2104. doi:10.1016/j.cub.2020.04.037

Silbering, A. F., Rytz, R., Grosjean, Y., Abuin, L., Ramdya, P., Jefferis, G. S., & Benton, R. (2011). Complementary function and integrated wiring of the evolutionarily distinct Drosophila olfactory subsystems. *J Neurosci, 31*(38), 13357-13375. doi:10.1523/JNEUROSCI.2360-11.2011

Strutz, A., Soelter, J., Baschwitz, A., Farhan, A., Grabe, V., Rybak, J., . . . Sachse, S. (2014). Decoding odor quality and intensity in the Drosophila brain. *Elife, 3*, e04147. doi:10.7554/eLife.04147

Sullivan, R. M. (2003). Developing a sense of safety: the neurobiology of neonatal attachment. *Ann N Y Acad Sci, 1008*, 122-131. Retrieved from http://www.ncbi.nlm.nih.gov/pubmed/14998878

Talay, M., Richman, E. B., Snell, N. J., Hartmann, G. G., Fisher, J. D., Sorkac, A., . . . Barnea, G. (2017). Transsynaptic Mapping of Second-Order Taste Neurons in Flies by trans-Tango. *Neuron, 96*(4), 783-795 e784. doi:10.1016/j.neuron.2017.10.011

Tsao, C. H., Chen, C. C., Lin, C. H., Yang, H. Y., & Lin, S. (2018). Drosophila mushroom bodies integrate hunger and satiety signals to control innate food-seeking behavior. *Elife, 7*. doi:10.7554/eLife.35264

Walker, S. J., Corrales-Carvajal, V. M., & Ribeiro, C. (2015). Postmating Circuitry Modulates Salt Taste Processing to Increase Reproductive Output in Drosophila. *Curr Biol*. doi:10.1016/j.cub.2015.08.043

Woller, A., Bandow, P., Aimon, S., & Grunwald Kadow, I. C. (2021). Preparing Adult Drosophila melanogaster for Whole Brain Imaging during Behavior and Stimuli Responses. *J Vis Exp*(170). doi:10.3791/61876

Yapici, N., Kim, Y. J., Ribeiro, C., & Dickson, B. J. (2008). A receptor that mediates the post-mating switch in Drosophila reproductive behaviour. *Nature, 451*(7174), 33-37. doi:10.1038/nature06483

Zhao, M., Garland, T., Jr., Chappell, M. A., Andrew, J. R., & Saltzman, W. (2017). Metabolic and affective consequences of fatherhood in male California mice. *Physiol Behav, 177*, 57-67. doi:10.1016/j.physbeh.2017.04.010

Zhao, X., Lenek, D., Dag, U., Dickson, B. J., & Keleman, K. (2018). Persistent activity in a recurrent circuit underlies courtship memory in Drosophila. *Elife, 7*. doi:10.7554/eLife.31425

Figures and Figure legends

Figure 1. Odor experience at mating changes female attraction to polyamines

(A) Scheme depicting paradigm used in all experiments. Virgin females were kept alone for 6-7 days or mated on day 2 for 24 h, then separated, and test at day 6-7 for their preference for the odor of the polyamine, putrescine. Mated females show a high preference for polyamine, which depends on mating-induced modulation of polyamine-detecting olfactory neurons (see text for details). (B) CantonS females before mating (virgins) and 1-9 days after mating (a.m.) were analyzed for their preference to putrescine odor as groups in a T-maze. (C) *In vivo* 2-photon imaging GCaMP-reported calcium levels in DANs innervating the MB. Note that cVA induces higher calcium increases in mated females as compared to virgins primarily in the β'1 compartment of the MB. (D) Graph showing the peak maxima of GCaMP signals induced in different MB compartments before and after mating. ANOVA, P-values: n.s.:>0.05, *: <0.05, **: <0.01, ***: <0.001 (E) Females mutant for ORCO (*ORCO*^{mutant}) showed a significantly reduced preference for polyamines during olfactory preference test compared to controls (*ORCO*^{het}). Note that ORCO is not required for the detection of polyamine odor, but for the detection of pheromones and other food related odors. T-maze group assay. Bars depict preference index (PI) ± SEM. Student-s t-test; P-values: n.s.:>0.05, *: <0.05, **: <0.01 (F) T-maze group assay for females mated at restrictive temperature (32ºC) and tested at permissive temperature for their polyamine preference (25ºC). In addition, ORCO>shi^{ts1} and pooled IR76b and IR41a-Gal4>shi^{ts1} females were mated and tested at 25ºC as a control. Note that synaptic inhibition of ORCO-expressing OSNs during mating significantly reduced the females' attraction to putrescine odor. T-maze group assay. (G) T-maze group assay for females mated at restrictive temperature (32ºC) or at permissive temperature (25ºC) and tested at permissive temperature for their polyamine preference (25ºC). Note that increased temperature at test leads to a slightly higher attraction to polyamine as compared to testing at 25ºC. This might explain why the difference between flies of the same genotype tested at different temperatures is reduced by not significantly. Bars depict preference index (PI) ± SEM. Student-s t-test; P-values: n.s.:>0.05, *: <0.05, **: <0.01. N > 8 groups of 20-40 female flies.

Figure 2. The mushroom body and learning mechanisms are required in long-term preference change upon mating.

(A) Scheme of experimental paradigm used to block Kenyon cell (KC) synaptic output at precise times during the experiment. Shibire^{ts1} was expressed under the control of MB10B-Gal4 in all Kenyon cells (KCs). Temperature shifts from 25 to 30°C at four different time points were used to inhibit KC output before, during, after mating and at test, respectively. At day 6-7 after mating, females were given the choice between the odor of water (control) and the odor of putrescine in a T-maze assay. (B) KC synaptic output is required during mating and during preference test. Inhibition of KC output in virgin females during test did not affect putrescine odor preference. Single female preference for putrescine in T-maze assay. 50% represents chance. Fisher's exact test. All p-values depict the comparison between the respective control (*pBDP-Gal4;UAS-shi*^{ts1}) and the text group (*MB10B-Gal4;UAS-shi*^{ts1}). P-values: n.s.:>0.1, *: <0.1, **: <0.05, ***: <0.001. n = 16 single female flies.

Figure 3. β'1 dopaminergic neuron activation can replace mating to induce higher polyamine preference.

(A) Activation of PAM-β'1 output (*MB188B-Gal4;UAS-dTrpA1*) instead of mating significantly increased virgin female preference for putrescine at the time of test. Vice versa, it significantly decreased the mated female's preference for the same at testing. (B) Inhibition of PAM-β'1 dopaminergic neuron output

(*MB188B-Gal4;UAS-shi^{ts1}*) during or instead of mating had no significant effect on mated or virgin female preference for putrescine at the time of test, respectively. (C) Activation of PPL1 dopaminergic neuron output (*MB60B-Gal4;UAS-dTrpA1*) during mating reduced mated female preference for putrescine at the time of test. (D) Inhibition of PAM dopaminergic neuron output (*MB316B-Gal4;UAS-shi^{ts1}*) during test significantly decreased mated female preference for putrescine at the time of test. Single female preference for putrescine in T-maze assay. 50% represents chance. Fisher's exact test; All p-values depict the comparison between the respective control (*pBDP-Gal4;UAS-xx*) and the text group (*MBx-Gal4;UAS-xx*). P-values: n.s.:>0.1, *: <0.1, **: <0.05, ***: <0.001. n = 16 single female flies.

Figure 4. β'1 mushroom body output at mating regulates polyamine preference
(A) Inhibition of MBON-β'1 output (*MB57B-Gal4;UAS-shi^{ts1}*) during mating significantly reduced mated female preference for putrescine at the time of test. Single female preference for putrescine in T-maze assay. 50% represents chance. (B) Activation MBON-β'1 output (*MB57B-Gal4;UAS-dTrpA1*) instead of mating significantly increased virgin female preference for putrescine at the time of test. (C) Neuronal output was inhibited during preference test. Inhibition of MBON-β'1 output (*MB57B-Gal4;UAS-shi^{ts1}*) at the time of test had no influence on virgin female preference for putrescine. (D) Activation of MBON-β'2 output (*MB11B-Gal4;UAS-dTrpA1*) during test significantly reduced mated female preference for putrescine. (E) Activation MBON-β'2 output (*MB11B-Gal4;UAS-dTrpA1*) instead of or during mating did not change female preference for putrescine at the time of test. (F) Inhibition of MBON-β'2 output (*MB11B-Gal4;UAS-shi^{ts1}*) during testing significantly increased virgin female preference for putrescine at the time of test. Single female preference for putrescine in T-maze assay. 50% represents chance. Fisher's exact test; All p-values depict the comparison between the respective control (*pBDP-Gal4;UAS-xx*) and the text group (*MBx-Gal4;UAS-xx*). P-values: n.s.:>0.1, *: <0.1, **: <0.05, ***: <0.001. n = 16 single female flies.

Figure 5. Odor responses of MBONs before and after mating
(A) Scheme depicting imaging plane through MBON-β'1. (B) GCaMP6f was expressed under the control of MB57B-Gal4 in β'1 MBONs. Dashed circle indicates the region of interest (ROI) used for quantification of the signal. (C) Representative image showing response of MBON-β'1 to putrescine. (D) Representative image showing the response of MBON-β'1 to cVA (11-cis-Vaccenyl Acetate). (E) Peak ΔF/F GCaMP signals in response to water, putrescine or cVA. Responses of virgins and mated females are shown. (F) Scheme depicting imaging plane through MBON-β'2. (G) GCaMP6f was expressed under the control of MB11B-Gal4 in β'2 MBONs. Dashed circle indicates the region of interest (ROI) used for quantification of the signal. (H) Representative image showing response of MBON-β'2 to putrescine. (I) Representative image showing the response of MBON-β'2 to cVA (cis-Vaccenyl Acetate). (J) Peak ΔF/F GCaMP signals in response to water, putrescine or cVA. Responses of virgins and mated females are shown. ANOVA, P-values: n.s.:>0.05, *: <0.05, **: <0.01, ***: <0.001

Figure 6. Lateral horn pathway contributes to the expression of polyamine attraction.
(A) *In vivo* whole brain lightfield calcium imaging upon stimulation with putrescine or vinegar (*nsyb-Gal4; UAS-GCaMP6m*). Putrescine and vinegar activate different areas in the lateral horn (LH, dotted line). (B) Electron microscopy (EM)-based reconstruction showing projection neurons (PN) innervating the VC5 glomerulus. (C) VC5 PNad (pink) innervates the LH and the mushroom body (MB). (D) LH output neuron (LHON) AD1b2 is the main downstream partner of VC5 PNad. (E) T-maze behavioral screen at restrictive temperature at test (30ºC) of candidate LHONs in mated females reveals that two LHON types are required for full attraction to putrescine. 'emptyxshi' represents the control group and stands for *pBDPGAL4;UAS-*

shi^{ts1}, the Gal4 vector used to generate all MB-Gal4 lines without an expression driving enhancer. (F) One-way Anova, Bonferroni corrected; P-values: *: <0.05. (F) LHON AD1b2 is directly and indirectly synaptically connected to PAM-DANs innervating the β'1 compartment of the mushroom body. LH: Lateral horn, Cx: Mushroom body calyx, AL: Antennal lobe

Figure 7. The mushroom body regulates odor preference behavior of females before and after mating. Working model showing that in virgin females (before mating), the activity of PPL1 dopaminergic neurons and MBONβ'2 suppress the expression of polyamine odor preference. During mating, β'1 PAM dopaminergic neurons and β'1 convey the experience of mating, possibly through the detection of the pheromone cVA, to the mushroom body. This mechanism induces a long-lasting change in polyamine preference in mating females. After mating, mated females express their higher attraction to polyamine odor through a circuit involving the activity of PAM-β'2,γ4 dopaminergic neurons and the suppression of MBON-β'2 output. In addition, output of the lateral horn through at least two different types of output neurons (AD1b2 and aSP-g) is required for the expression of high polyamine preference. It is conceivable that the lateral horn and the mushroom body circuits are connected through specific output or modulatory neurons.

Supplementary figures

Figure S1 related to Figure 1.
(A) Mating does not increase the attraction of females to different concentrations of ammonia. (B) Seminal fluid is not required to induce postmating polyamine preference. Wildtype CantonS females were mated with males without seminal fluid (*prd-Gal4;UAS-BiP RNAi*) or with control males (*prd-Gal4/+* or *UAS-BiP RNAi/+*). (C) Sperm is not essential for postmating polyamine preference induction. Wildtype CantonS females were mated with sterile males unable to produce sperm (sons of *tudor*-deficient females) or with control males (control). Single female preference for putrescine in T-maze assay. 50% represents chance. (D) Egg production does not drive female's increased preference for polyamines. Mated females unable to produce eggs (ovoD) behaved no different from control females producing eggs. Single female preference for putrescine in T-maze assay. 50% represents chance. (E) Courtship without mating induces higher preference in virgin females. Note that preference of courted, not mated virgins is not significantly different from mated females (p>0.1). Single female preference for putrescine in T-maze assay. 50% represents chance. (F) Wildtype CantonS females were exposed in food vials for 24 h to water or to cVA (pure) and then tested in the T-maze assay for their preference for putrescine. No significant difference was found between the two groups. (G) Standard fly food contains high levels of polyamines, spermine, spermidine and putrescine. (H) Wildtype CantonS females were mated to wildtype males on different substrates. Mating for 24 h on pure agarose reduced mated female attraction to polyamines. Females behaved not significantly different from virgins (a, p>0.1) and females mated on regular fly food (b, p>0.1). Single female preference for putrescine in T-maze assay. 50% represents chance. (I) Group T-maze preference assay with females raised and mated on holidic diet or standard fly food. No significant difference was found between the groups. Depicted p-values for single fly assay, unless indicated otherwise, refer to the difference between experimental and control group in virgins or mated females, respectively. Fisher's exact test. P-values: n.s.:>0.1, *: <0.1, **: <0.05, ***: <0.01. T-maze group assay. Bars depict preference index (PI) ± SEM. Student-s t-test; P-values: n.s.:>0.05, *: <0.05, **: <0.01.

Figure S2 related to Figure 2.
(A) Schematic overview of whole brain lightfield imaging method. For details see (Aimon et al., 2019) (B-E) Peak GCaMP fluorescence (ΔF/F) and regression analysis (R-square) of *in vivo* calcium whole brain lightfield imaging reveals no global differences in brain state or brain region activity between virgin and mated females (ANOVA).

Figure S3 related to Figure 3.
(A) left, schematic representation and description of PAM neuron transgenic lines. right, scheme of experimental paradigm. Neuronal output was blocked during odor preference test. (B) Inhibition of PAM dopaminergic neuron output (*MB42B-Gal4;UAS-shi^{ts1}*) during test significantly decreased mated female preference for putrescine at the time of test. Single female preference for putrescine in T-maze assay. 50% represents chance. (C) Inhibition of PAM dopaminergic neuron output (*MB109B-Gal4;UAS-shi^{ts1}*) during test had no significant effect on mated female preference for putrescine at the time of test. Single female preference for putrescine in T-maze assay. 50% represents chance. (D) Activation of PAM dopaminergic neuron output (*MB109B-Gal4;UAS-shi^{ts1}*) during or instead of mating had no significant effect on mated or virgin female preference for putrescine at the time of test. Single female preference for putrescine in T-maze assay. 50% represents chance. (E) EM-based connectome showing synaptic connections of PAM-β'1 neurons. (F) left, scheme of PPL1 cluster of dopaminergic neurons and expression of three different transgenic lines. right, scheme showing experimental paradigm. Neuronal output was inhibited at the time of olfactory test. (G) Inhibition of PPL1-α'2α2 output (*MB58B-Gal4;UAS-shi^{ts1}*) during testing significantly increased virgin female preference for putrescine at the time of test. Single female preference for putrescine in T-maze assay. 50% represents chance. (H) Inhibition of PPL1-α'2α2, α3, γ2α'1 output (*MB60B-Gal4;UAS-shi^{ts1}*) during testing also significantly increased virgin female preference for putrescine at the time of test. Single female preference for putrescine in T-maze assay. 50% represents chance. (I) Inhibition of PPL1-α'2α2, α3, γ1pedc output (*MB438B-Gal4;UAS-shi^{ts1}*) during testing significantly increased virgin female preference for putrescine at the time of test. Single female preference for putrescine in T-maze assay. 50% represents chance. All p-values depict the comparison between the respective control (*pBDP-Gal4;UAS-shi^{ts1}*) and the text group (*MB10B-Gal4;UAS-shi^{ts1}*). P-values: n.s.:>0.1, *: <0.1, **: <0.05, ***: <0.001. n = 16 single female flies.

Figure S4 related to Figure 4.
(A) Activation MBON-β'1 output (*MB57B-Gal4;UAS-dTrpA1*) during testing significantly increased virgin female preference and decreased mated female preference for putrescine at the time of test, respectively. T-maze group assay. (B) Inhibition MBON-β'1 output (*MB57B-Gal4;UAS-shi^{ts1}*) during testing did not change mated female behavior. T-maze group assay. Bars depict preference index (PI) ± SEM. Student-s t-test; P-values: n.s.:>0.05, *: <0.05, **: <0.01. (C) Activation MBON-β'2 output (*MB11B-Gal4;UAS-dTrpA1*) instead of or during mating did not change female preference for putrescine at the time of test. Single female preference for putrescine in T-maze assay. 50% represents chance. P-values depict the comparison between the respective control (*pBDP-Gal4;UAS-shi^{ts1}*) and the text group (*MB10B-Gal4;UAS-shi^{ts1}*). P-values: n.s.:>0.1, *: <0.1, **: <0.05, ***: <0.001. n = 16 single female flies. (D) Reconstruction of neuronal morphology of MBON-β'1 (MBON10) and a PAM-β'2ma DAN in the MB. Trans-TANGO experiment reveals a possible direct synaptic connection between MBON-β'1 and MBON-β'2. Grey, anti-Ncad stains neuropil, green, anti-GFP shows expression in MBON-β'1, magenta, anti-dsred stains expression of trans-TANGO mediated expression of dsRed in synaptically connected MBON-β'2. (E') Higher magnification of images shown in (E). (F) MBON-β'1 form direct synaptic connections with PAM- β'2 DANs.

Figure S5 related to Figure 5.

Left panel shows the expression of GCaMP7f under the control of VT1211 in β'1/2 MBONs. The same flies express CsChrimson under the control of MB188B. Middle panel shows a representative image of a response to putrescine odor. Right graph shows the peak ΔF/F GCaMP responses in β'1 and 2 MBONs in three different groups of flies of the same genotype (*VT1211-GCaMP6f;MB188B-CsChrimson*). Flies were fed with retinal but not exposed to light (black bar), exposed to red light (white bar) or fed with retinal and exposed to red light (test group, yellow bar). No significant difference was found between the groups.

Figure S6 related to Figure 6.

(A) Trans-TANGO experiment reveals projection neurons (PNs) connecting the VC5 glomerulus to mushroom body (calyx) and lateral horn (LH). Grey, anti-Ncad stains neuropil, green, anti-GFP shows expression in IR76b neurons (IR76b>mCD8GFP), magenta, anti-dsred stains expression of trans-TANGO mediated expression of dsRed in synaptically connected neurons including PNs. (B) Trans-TANGO experiment reveals projection neurons (PNs) connecting the VC5 glomerulus to mushroom body (calyx) and lateral horn (LH). Grey, anti-Ncad stains neuropil, green, anti-GFP shows expression in IR76b neurons (IR41a>mCD8GFP), magenta, anti-dsred stains expression of trans-TANGO mediated expression of dsRed in synaptically connected neurons including PNs. (B') Higher magnification of images shown in (B). (C) NeuPrint-generated connectome of VC5 adPN and its synaptic connections to the LHON AD1b2. (D) EM-Reconstruction. LHON aSP-g receives input from the DA1 PN. Note that the DA glomerulus is responds to the pheromone cVA. (E) mCD8-GFP expression driven by Split-Gal4 lines L1538. (F) mCD8-GFP expression driven by Split-Gal4 lines L1539. (G) mCD8-GFP expression driven by Split-Gal4 lines L1779. (H) NeuPrint-generated connectome between VC5/polyamine sensitive ORNs and PAM-β'1. (I) NeuPrint-generated connectome between VC5/polyamine sensitive ORNs and PAM-β'1.

Figure S7 related to Figure 7.

(A) top, scheme of MBON-α2sc and expression of line MB80C. bottom, scheme showing experimental paradigm. Neuronal output was blocked at the time of preference test. (B) Inhibition of MBON-α2sc output (*MB80C-Gal4;UAS-shi*^{ts1}) at the time of test significantly reduced mated female preference for putrescine. T-maze group assay. Bars depict preference index (PI) ± SEM. Student's t-test; **<0.01

Figure 1

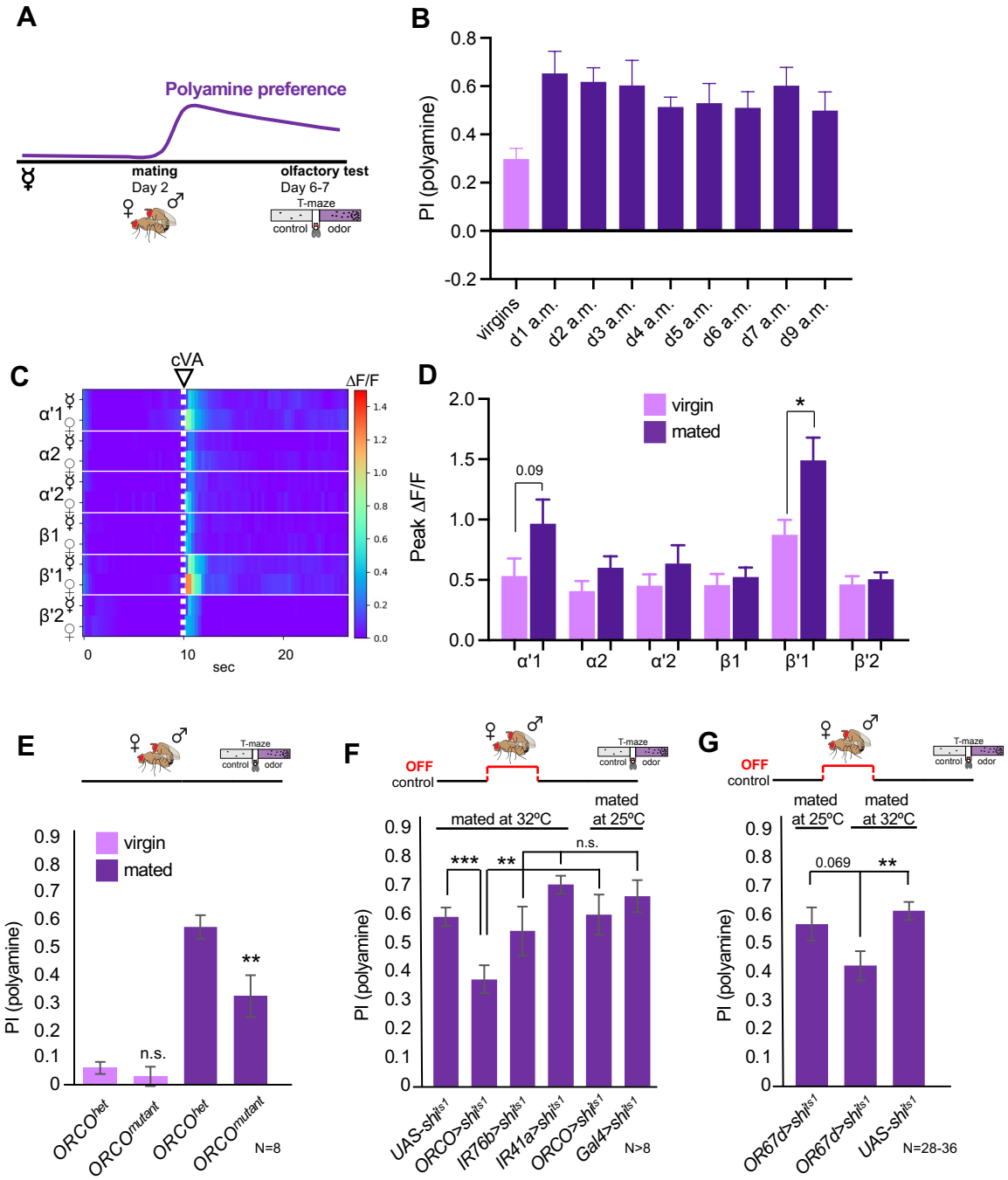
A
Polyamine preference
mating
Day 2
olfactory test
Day 6-7
T-maze
control
odor
B
PI (polyamine)
virgins
d1 a.m.
d2 a.m.
d3 a.m.
d4 a.m.
d5 a.m.
d6 a.m.
d7 a.m.
d9 a.m.
C
cVA
ΔF/F
α'1
α2
α'2
β1
β'1
β'2
sec
D
virgin
mated
Peak ΔF/F
0.09
*
E
virgin
mated
PI (polyamine)
n.s.
**
ORCO^het
ORCO^mutant
N=8
F
OFF
control
mated at 32ºC
mated at 25ºC
***
**
n.s.
UAS-shi^ts1
ORCO>shi^ts1
IR76b>shi^ts1
IR41a>shi^ts1
Gal4>shi^ts1
N>8
G
mated at 25ºC
mated at 32ºC
0.069
OR67d>shi^ts1
UAS-shi^ts1
N=28-36

Figure S1

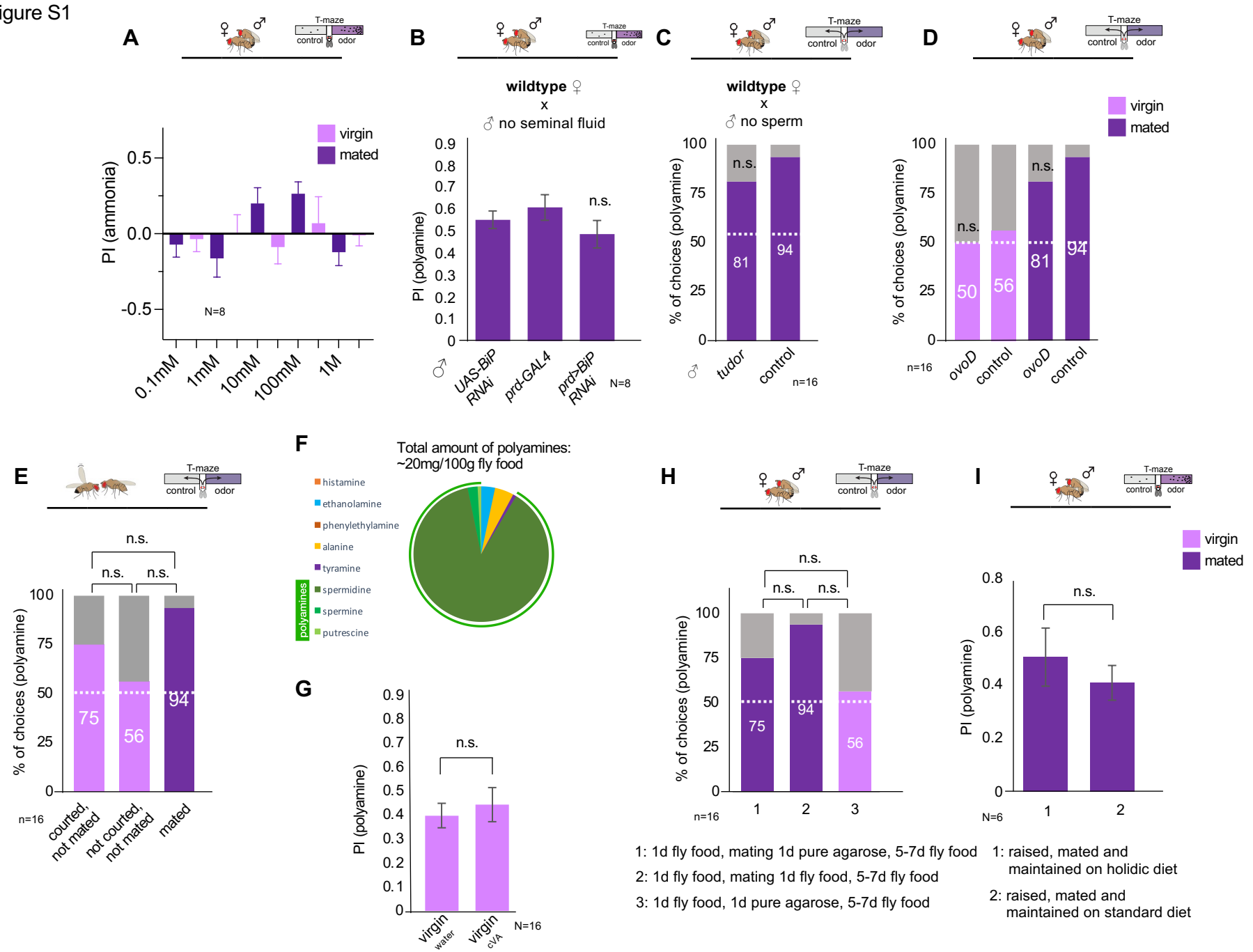
A
B
C
D
E
F
G
H
I
T-maze
control
odor
virgin
mated
PI (ammonia)
N=8
0.1mM
1mM
10mM
100mM
1M
wildtype ♀
x
♂ no seminal fluid
PI (polyamine)
n.s.
♂ UAS-BiP RNAi
prd-GAL4
prd>BiP RNAi
N=8
wildtype ♀
x
♂ no sperm
% of choices (polyamine)
81
94
♂ tudor
control
n=16
50
56
ovoD
n=16
75
courted, not mated
not courted, not mated
mated
Total amount of polyamines:
~20mg/100g fly food
histamine
ethanolamine
phenylethylamine
alanine
tyramine
spermidine
spermine
putrescine
polyamines
virgin water
virgin cVA
N=16
N=6
1: 1d fly food, mating 1d pure agarose, 5-7d fly food
2: 1d fly food, mating 1d fly food, 5-7d fly food
3: 1d fly food, 1d pure agarose, 5-7d fly food
1: raised, mated and maintained on holidic diet
2: raised, mated and maintained on standard diet

Figure 2

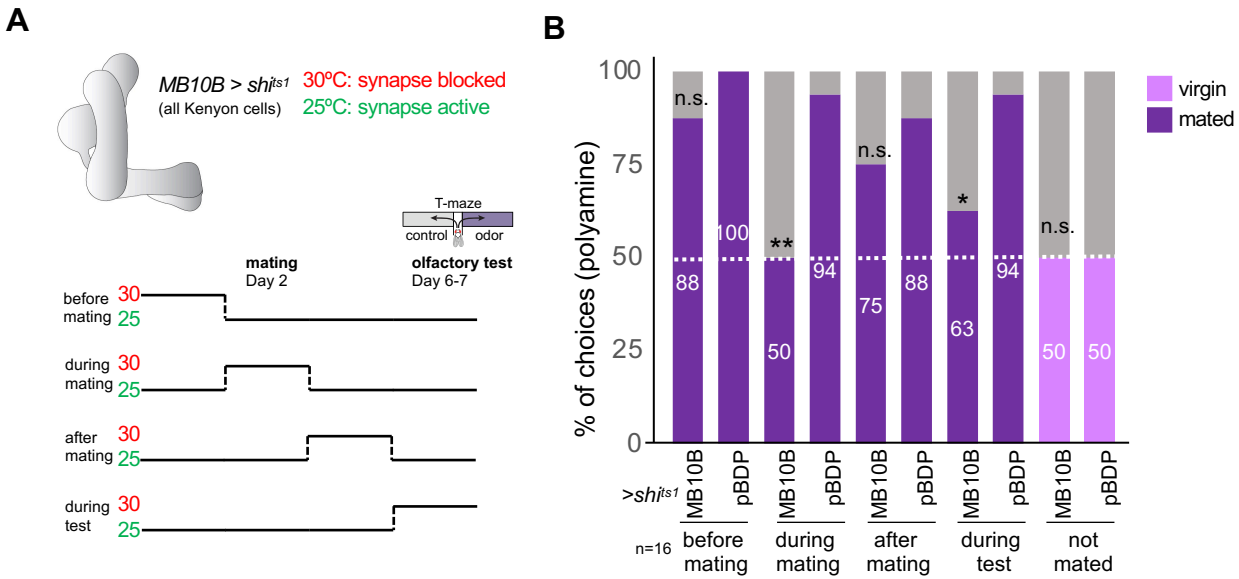
A
MB10B > shits1
(all Kenyon cells)
30ºC: synapse blocked
25ºC: synapse active
T-maze
control
odor
mating
Day 2
olfactory test
Day 6-7
before mating
during mating
after mating
during test
30
25
B
% of choices (polyamine)
100
75
50
25
0
virgin
mated
n.s.
**
*
88
100
50
94
75
88
63
94
50
50
>shits1
MB10B
pBDP
n=16
before mating
during mating
after mating
during test
not mated

Figure S2

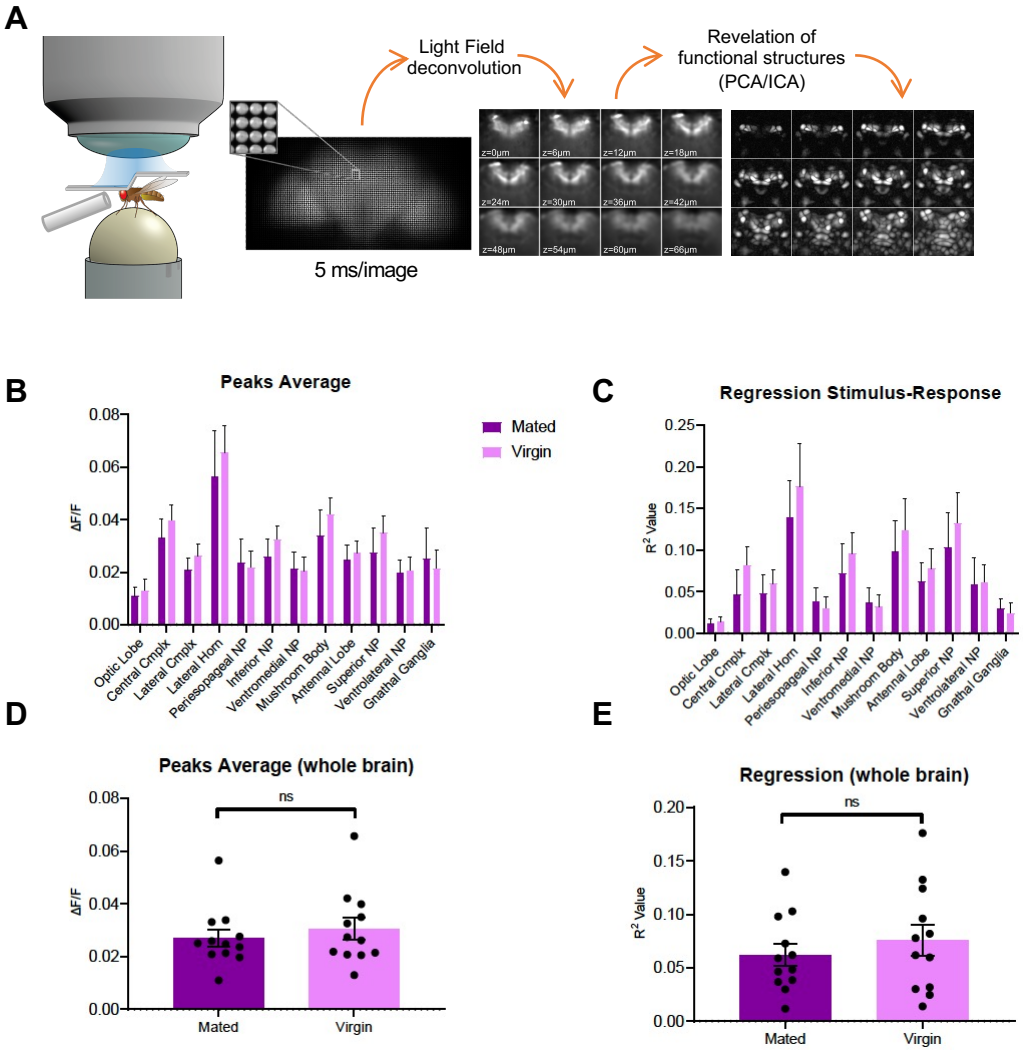
A
Light Field deconvolution
Revelation of functional structures (PCA/ICA)
5 ms/image
B
Peaks Average
Mated
Virgin
ΔF/F
Optic Lobe
Central Cmplx
Lateral Cmplx
Lateral Horn
Periesopageal NP
Inferior NP
Ventromedial NP
Mushroom Body
Antennal Lobe
Superior NP
Ventrolateral NP
Gnathal Ganglia
C
Regression Stimulus-Response
R² Value
D
Peaks Average (whole brain)
ns
Mated
Virgin
E
Regression (whole brain)

Figure 3

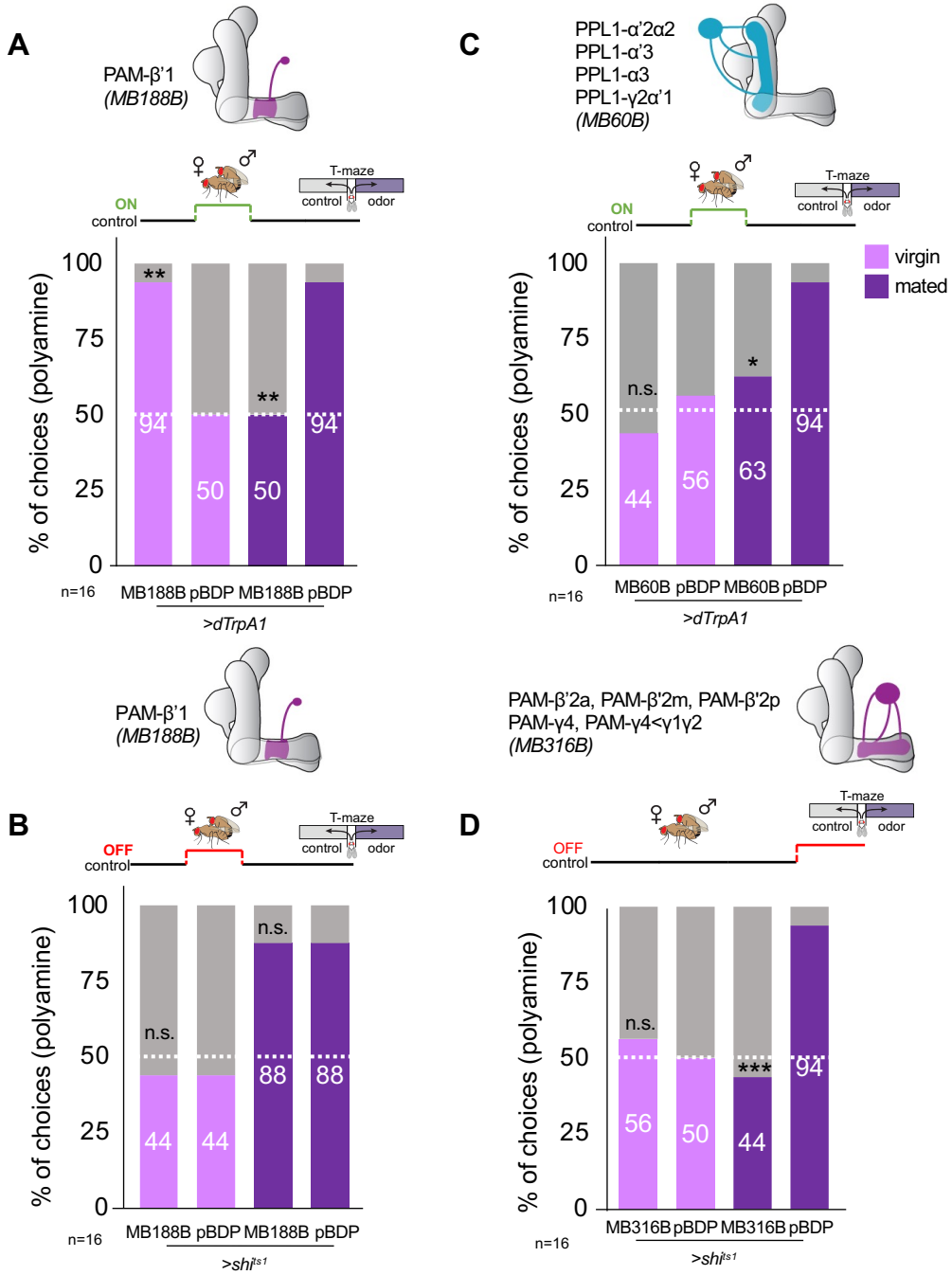
A
PAM-β'1
(MB188B)
ON
control
T-maze
control
odor
% of choices (polyamine)
100
75
50
25
0
**
94
50
**
50
94
n=16
MB188B pBDP MB188B pBDP
>dTrpA1
C
PPL1-α'2α2
PPL1-α'3
PPL1-α3
PPL1-γ2α'1
(MB60B)
ON
control
T-maze
control
odor
virgin
mated
n.s.
44
56
*
63
94
MB60B pBDP MB60B pBDP
>dTrpA1
PAM-β'1
(MB188B)
B
OFF
control
T-maze
control
odor
n.s.
44
44
n.s.
88
88
MB188B pBDP MB188B pBDP
>shi^ts1
PAM-β'2a, PAM-β'2m, PAM-β'2p
PAM-γ4, PAM-γ4<γ1γ2
(MB316B)
D
OFF
control
T-maze
control
odor
n.s.
56
50
***
44
94
MB316B pBDP MB316B pBDP
>shi^ts1

Figure S3

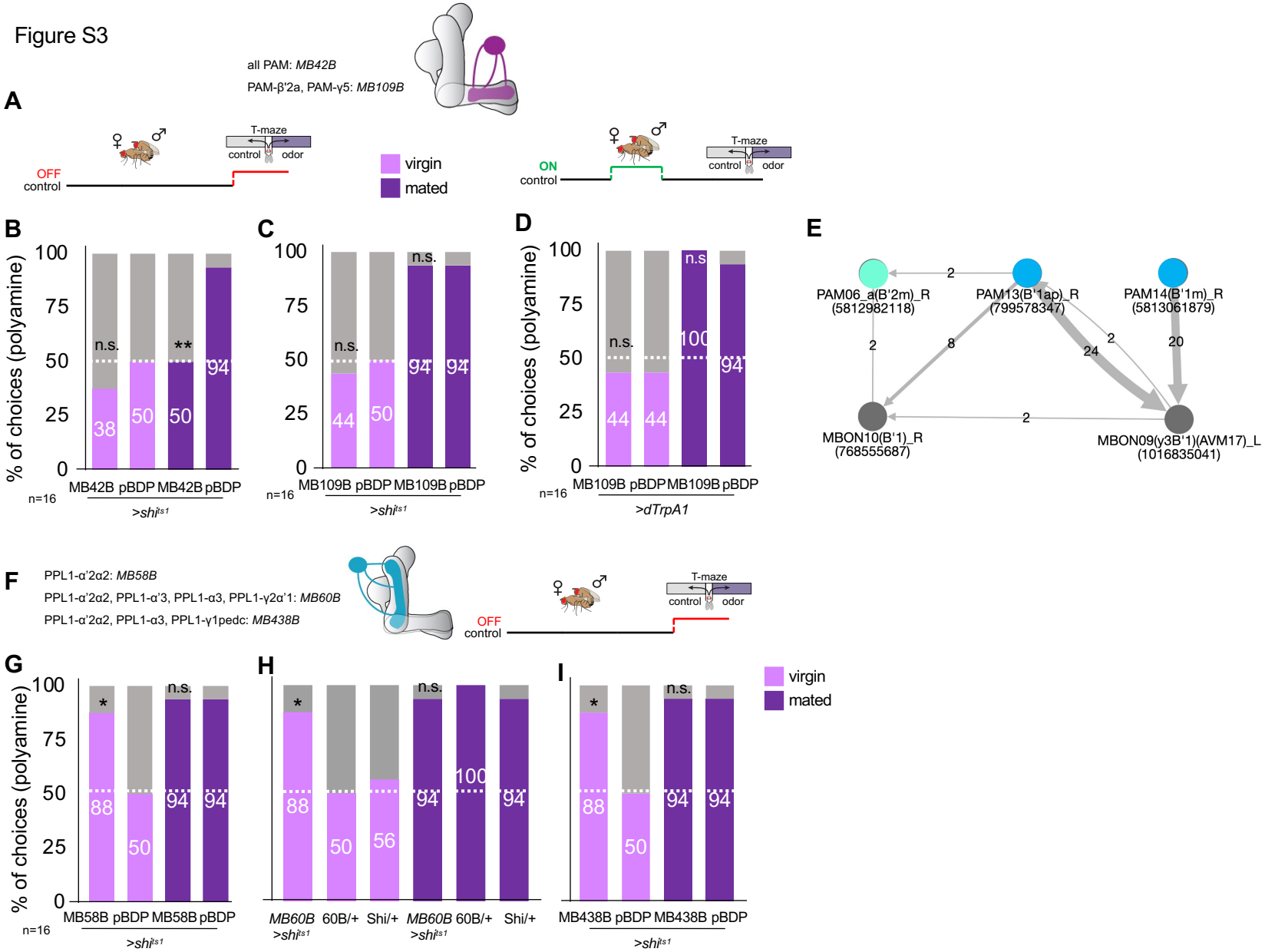
all PAM: MB42B
PAM-β'2a, PAM-γ5: MB109B
A
OFF
control
T-maze
control
odor
virgin
mated
ON
control
B
% of choices (polyamine)
n.s.
**
38
50
50
94
MB42B pBDP MB42B pBDP
n=16
>shi^ts1
C
n.s.
44
50
94
94
MB109B pBDP MB109B pBDP
D
n.s
100
44
44
94
>dTrpA1
E
PAM06_a(B'2m)_R
(5812982118)
PAM13(B'1ap)_R
(799578347)
PAM14(B'1m)_R
(5813061879)
MBON10(B'1)_R
(768555687)
MBON09(y3B'1)(AVM17)_L
(1016835041)
2
8
24
20
F
PPL1-α'2α2: MB58B
PPL1-α'2α2, PPL1-α'3, PPL1-α3, PPL1-γ2α'1: MB60B
PPL1-α'2α2, PPL1-α3, PPL1-γ1pedc: MB438B
G
*
88
50
94
94
MB58B pBDP MB58B pBDP
H
56
100
MB60B 60B/+ Shi/+ MB60B 60B/+ Shi/+
I
MB438B pBDP MB438B pBDP

Figure 4

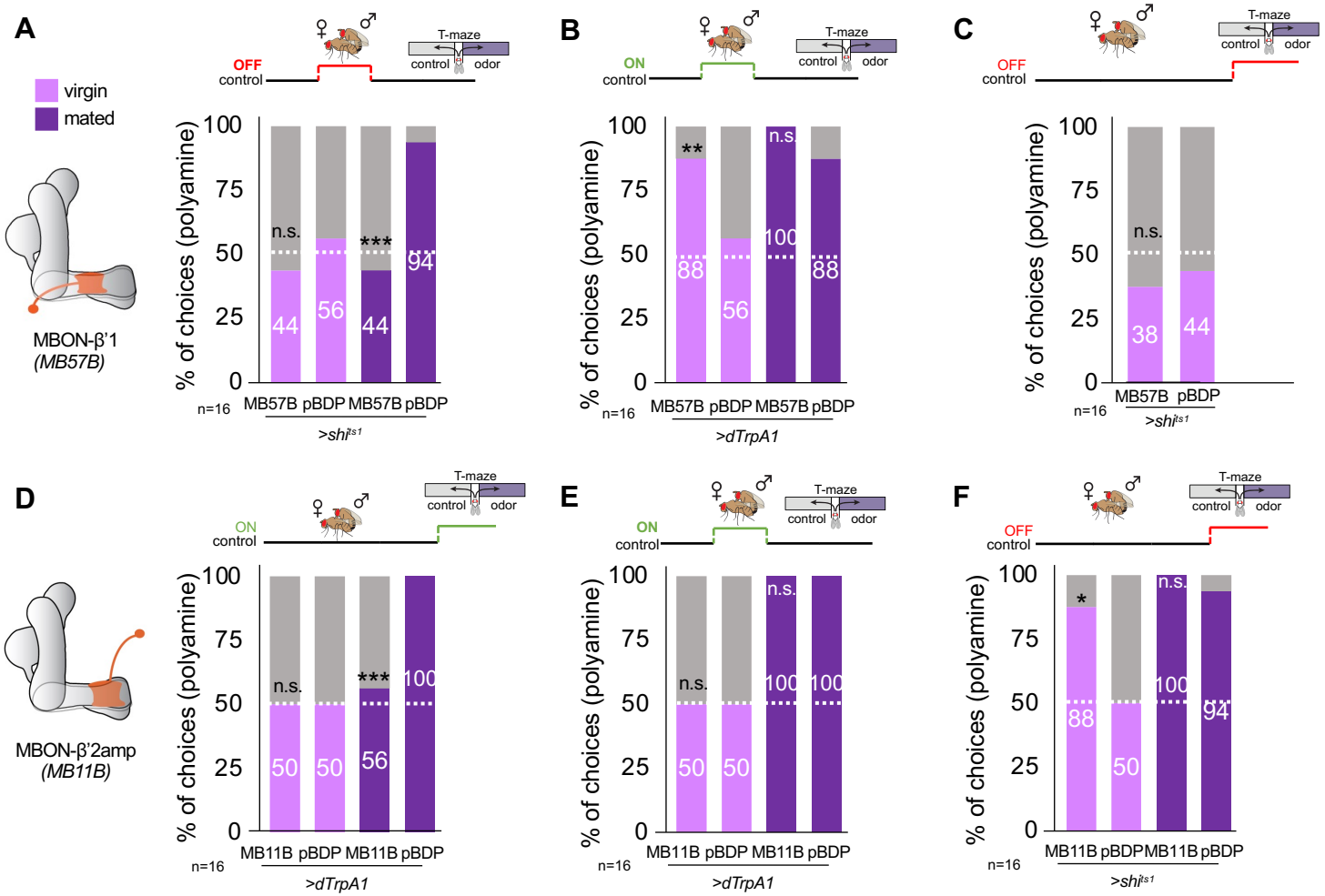
A
virgin
mated
MBON-β'1
(MB57B)
OFF
control
T-maze
control
odor
% of choices (polyamine)
100
75
50
25
0
n.s.
***
44
56
44
94
n=16
MB57B pBDP MB57B pBDP
>shi^ts1
B
ON
control
T-maze
control
odor
**
n.s.
88
56
100
88
MB57B pBDP MB57B pBDP
>dTrpA1
C
OFF
control
T-maze
control
odor
n.s.
38
44
MB57B pBDP
>shi^ts1
D
ON
control
T-maze
control
odor
MBON-β'2amp
(MB11B)
n.s.
***
50
50
56
100
MB11B pBDP MB11B pBDP
>dTrpA1
E
ON
control
T-maze
control
odor
n.s.
n.s.
50
50
100
100
MB11B pBDP MB11B pBDP
>dTrpA1
F
OFF
control
T-maze
control
odor
*
n.s.
88
50
100
94
MB11B pBDP MB11B pBDP
>shi^ts1

Figure S4

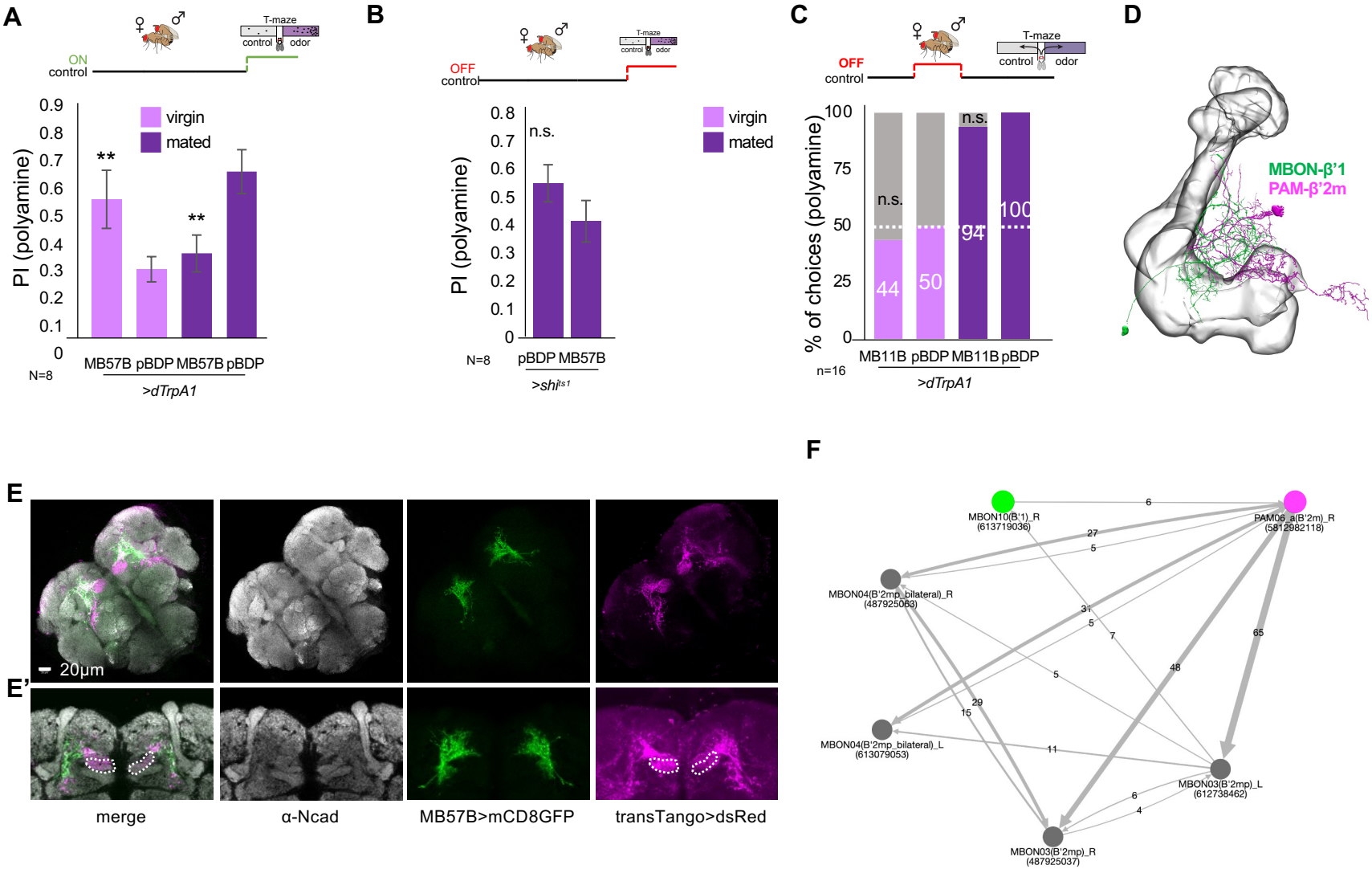
A
T-maze
control
odor
ON
control
PI (polyamine)
virgin
mated
**
**
MB57B pBDP MB57B pBDP
N=8
>dTrpA1
B
T-maze
control
odor
OFF
control
PI (polyamine)
n.s.
virgin
mated
N=8
pBDP MB57B
>shi^ts1
C
T-maze
control
odor
OFF
control
% of choices (polyamine)
n.s.
n.s.
44
50
94
100
MB11B pBDP MB11B pBDP
n=16
>dTrpA1
D
MBON-β'1
PAM-β'2m
E
20μm
E'
merge
α-Ncad
MB57B>mCD8GFP
transTango>dsRed
F
MBON10(B'1)_R
(613719036)
PAM06_a(B'2m)_R
(581298118)
MBON04(B'2mp_bilateral)_R
(487925083)
MBON04(B'2mp_bilateral)_L
(613079053)
MBON03(B'2mp)_L
(612738462)
MBON03(B'2mp)_R
(487925037)

Figure 5

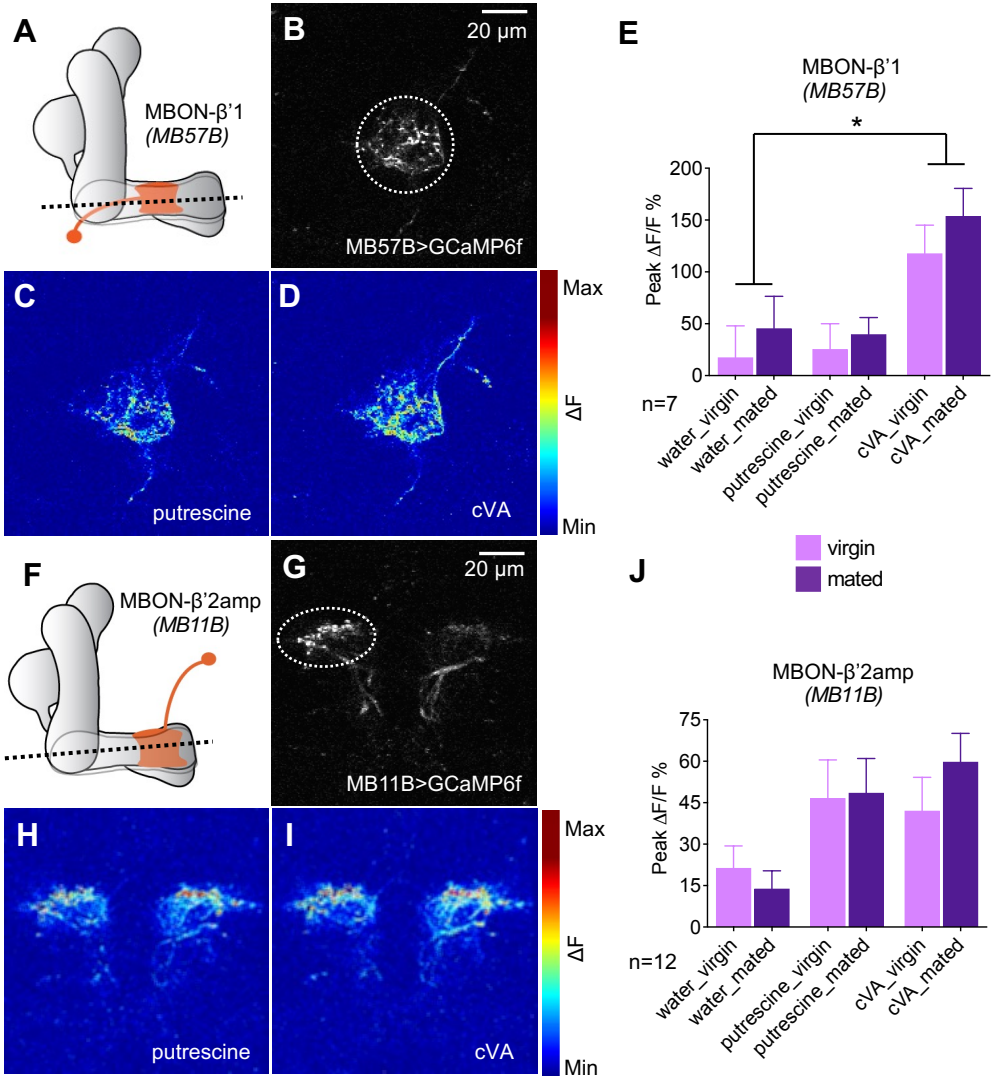
A
MBON-β'1
(MB57B)
B
20 µm
MB57B>GCaMP6f
C
putrescine
D
cVA
Max
ΔF
Min
E
MBON-β'1
(MB57B)
*
Peak ΔF/F %
200
150
100
50
0
n=7
water_virgin
water_mated
putrescine_virgin
putrescine_mated
cVA_virgin
cVA_mated
virgin
mated
F
MBON-β'2amp
(MB11B)
G
20 µm
MB11B>GCaMP6f
H
putrescine
I
cVA
Max
ΔF
Min
J
MBON-β'2amp
(MB11B)
Peak ΔF/F %
75
60
45
30
15
0
n=12
water_virgin
water_mated
putrescine_virgin
putrescine_mated
cVA_virgin
cVA_mated

Figure S5

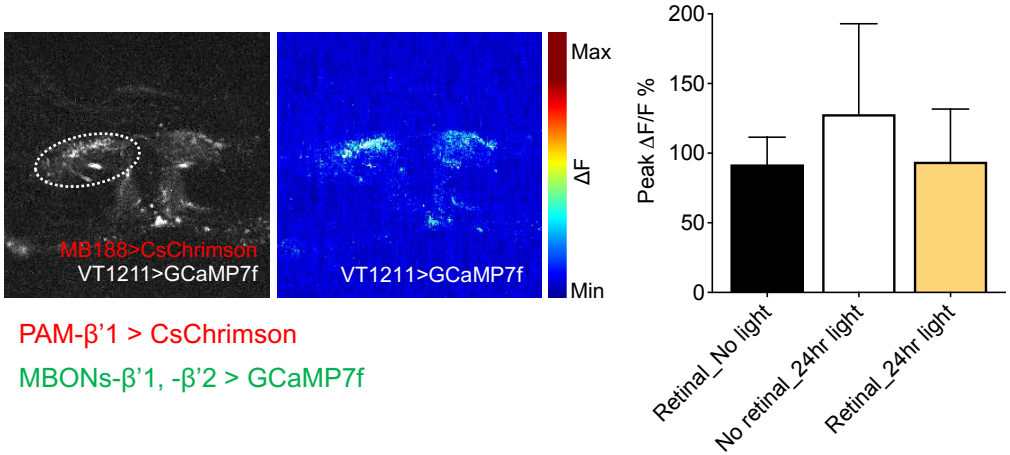

PAM-β'1 > CsChrimson

MBONs-β'1, -β'2 > GCaMP7f

Figure 6

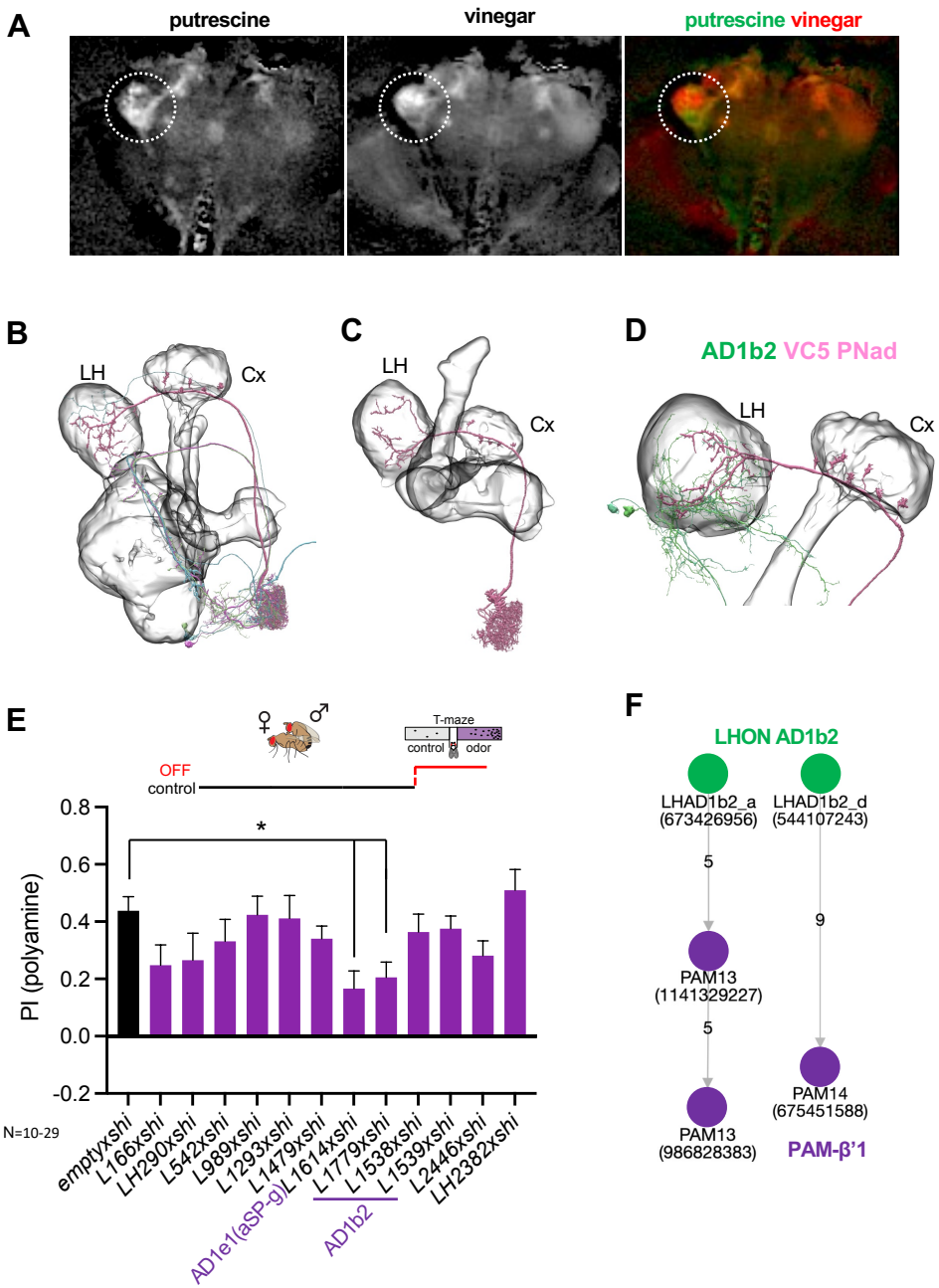
A
putrescine
vinegar
putrescine vinegar
B
LH
Cx
C
LH
Cx
D
AD1b2 VC5 PNad
LH
Cx
E
♀
♂
T-maze
control
odor
OFF
control
*
PI (polyamine)
0.8
0.6
0.4
0.2
0.0
-0.2
N=10-29
emptyxshi
L166xshi
LH290xshi
L542xshi
L989xshi
L1293xshi
L1479xshi
L1614xshi
L1779xshi
L1538xshi
L1539xshi
L2446xshi
LH2382xshi
AD1e1(aSP-g)
AD1b2
F
LHON AD1b2
LHAD1b2_a
(673426956)
LHAD1b2_d
(544107243)
5
9
PAM13
(1141329227)
5
PAM14
(675451588)
PAM13
(986828383)
PAM-β'1

Figure S6

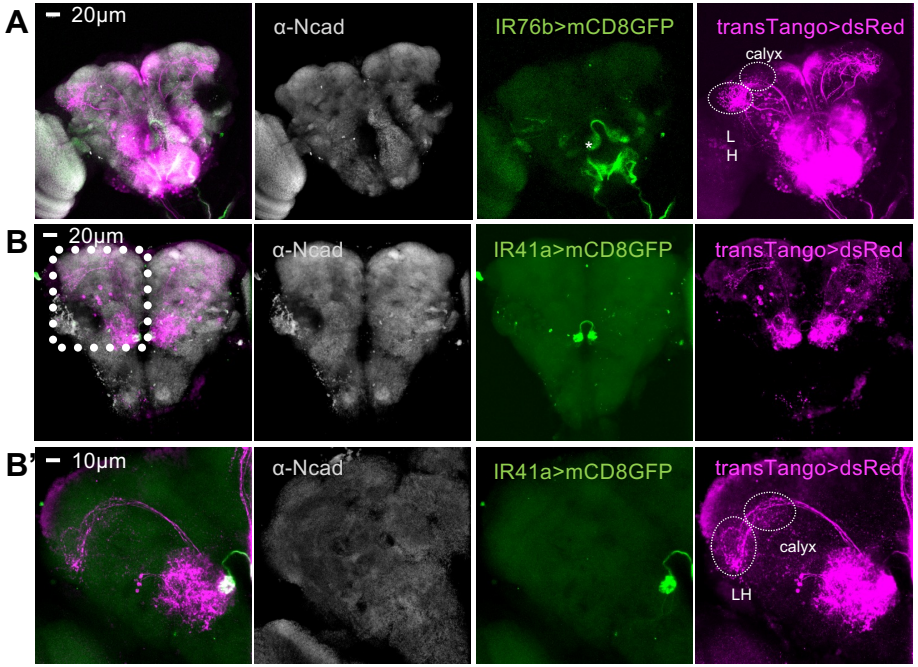
A
20μm
α-Ncad
IR76b>mCD8GFP
transTango>dsRed
calyx
L
H
B
20μm
α-Ncad
IR41a>mCD8GFP
transTango>dsRed
B'
10μm
α-Ncad
IR41a>mCD8GFP
transTango>dsRed
calyx
LH

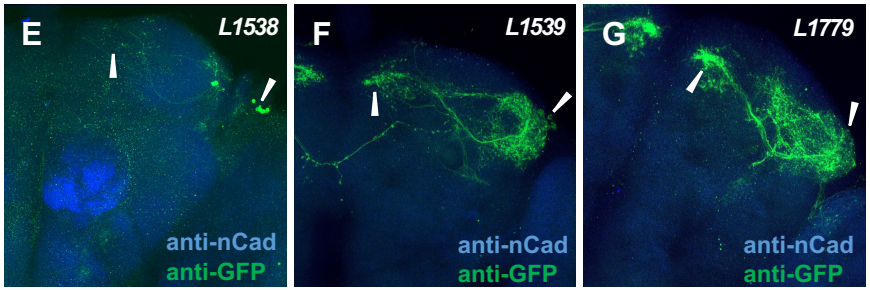
E
L1538
anti-nCad
anti-GFP
F
L1539
anti-nCad
anti-GFP
G
L1779
anti-nCad
anti-GFP

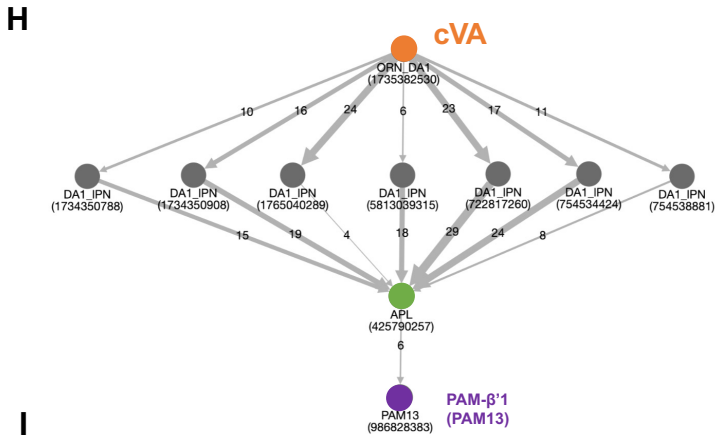
H
cVA
ORN_DA1
(1735382530)
DA1_lPN
(1734350788)
DA1_lPN
(1734350908)
DA1_lPN
(1765040289)
DA1_lPN
(5813039315)
DA1_lPN
(722817260)
DA1_lPN
(754534424)
DA1_lPN
(754538881)
APL
(425790257)
PAM13
(986828383)
PAM-β'1
(PAM13)

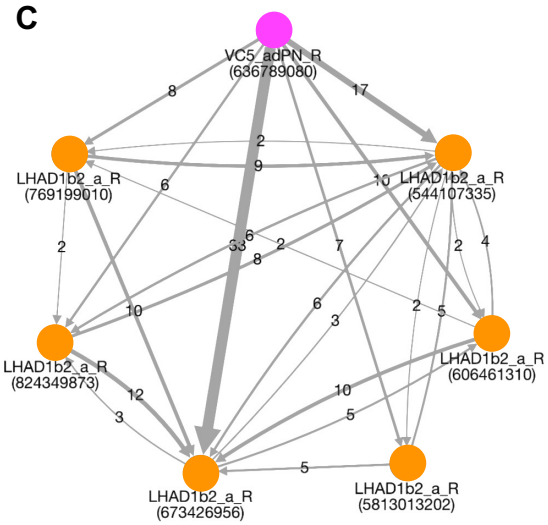
C
VC5_adPN_R
(636789080)
LHAD1b2_a_R
(769199010)
LHAD1b2_a_R
(544107335)
LHAD1b2_a_R
(824349873)
LHAD1b2_a_R
(606461310)
LHAD1b2_a_R
(673426956)
LHAD1b2_a_R
(5813013202)

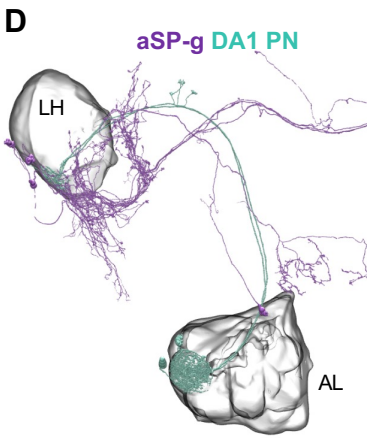
D
aSP-g DA1 PN
LH
AL

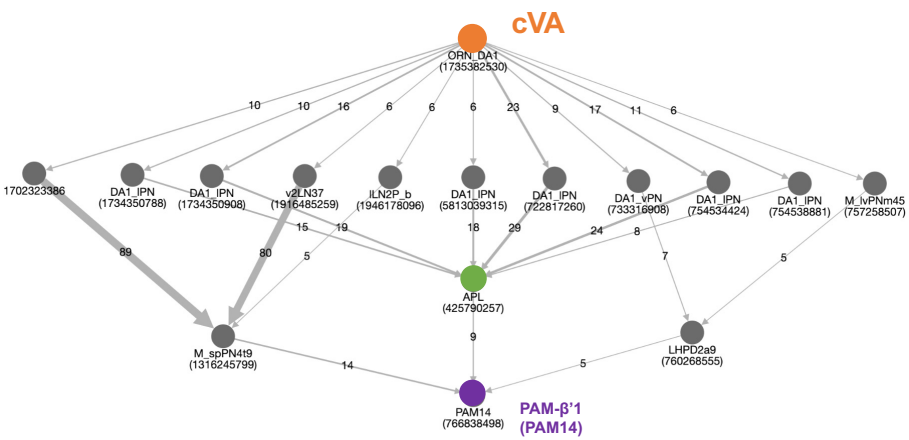
I
cVA
ORN_DA1
(1735382530)
1702323386
DA1_lPN
(1734350788)
DA1_lPN
(1734350908)
v2LN37
(1916485259)
lLN2P_b
(1946178096)
DA1_lPN
(5813039315)
DA1_lPN
(722817260)
DA1_vPN
(733316908)
DA1_lPN
(754534424)
DA1_lPN
(754538881)
M_lvPNm45
(757258507)
APL
(425790257)
M_spPN4t9
(1316245799)
LHPD2a9
(760268555)
PAM14
(766838498)
PAM-β'1
(PAM14)

Figure 7

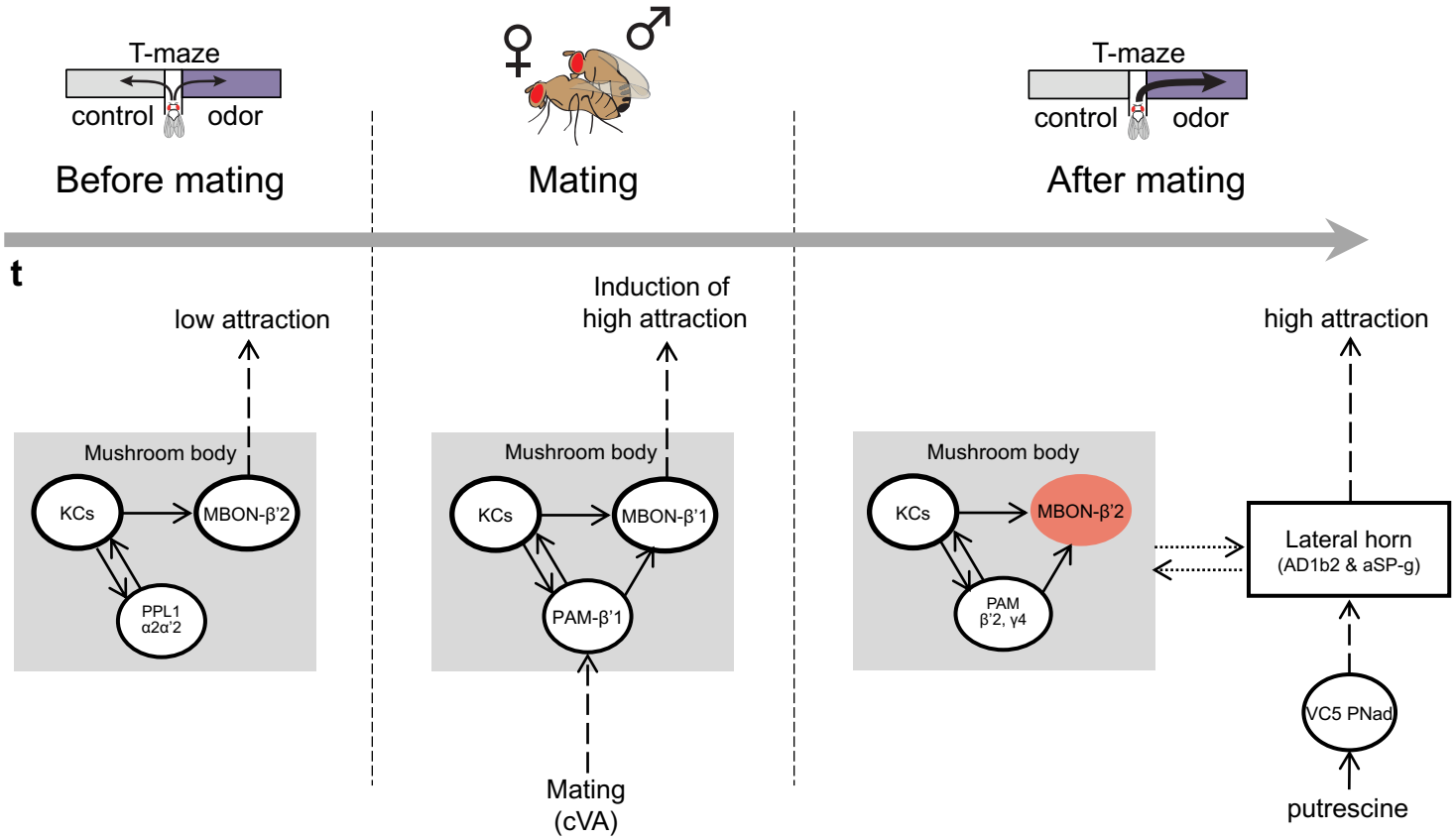
T-maze
control
odor
Before mating
♀
♂
Mating
T-maze
control
odor
After mating
t
low attraction
Mushroom body
KCs
MBON-β'2
PPL1
α2α'2
Induction of
high attraction
Mushroom body
KCs
MBON-β'1
PAM-β'1
Mating
(cVA)
Mushroom body
KCs
MBON-β'2
PAM
β'2, γ4
high attraction
Lateral horn
(AD1b2 & aSP-g)
VC5 PNad
putrescine

Figure S7

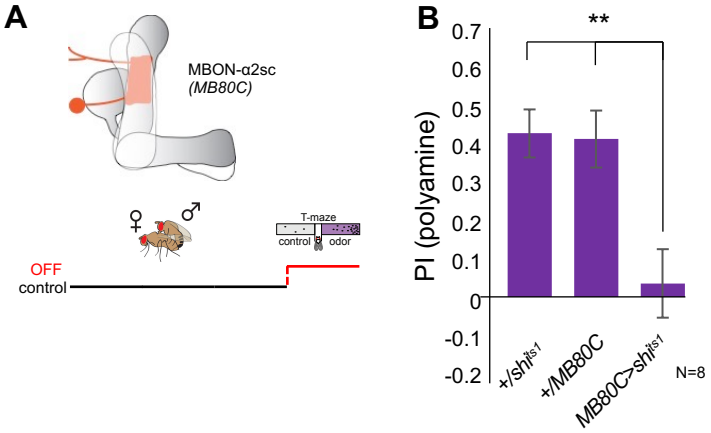
A
MBON-α2sc
(MB80C)
♀
♂
T-maze
control
odor
OFF
control
B
**
PI (polyamine)
0.7
0.6
0.5
0.4
0.3
0.2
0.1
0
-0.1
-0.2
+/shits1
+/MB80C
MB80C>shits1
N=8